AD-A044 169 WEIDLINGER ASSOCIATES NEW YORK F/G 9/2

THE POSSI CODE - A COMPUTER PROGRAM FOR A TWO-DIMENSIONAL PROBL--ETC(U)

MAR 77 A T MATTHEWS, H H BLEICH DNA001-76-C-0125

UNCLASSIFIED DNA-4299T NL

1 OF 1

ADA044169

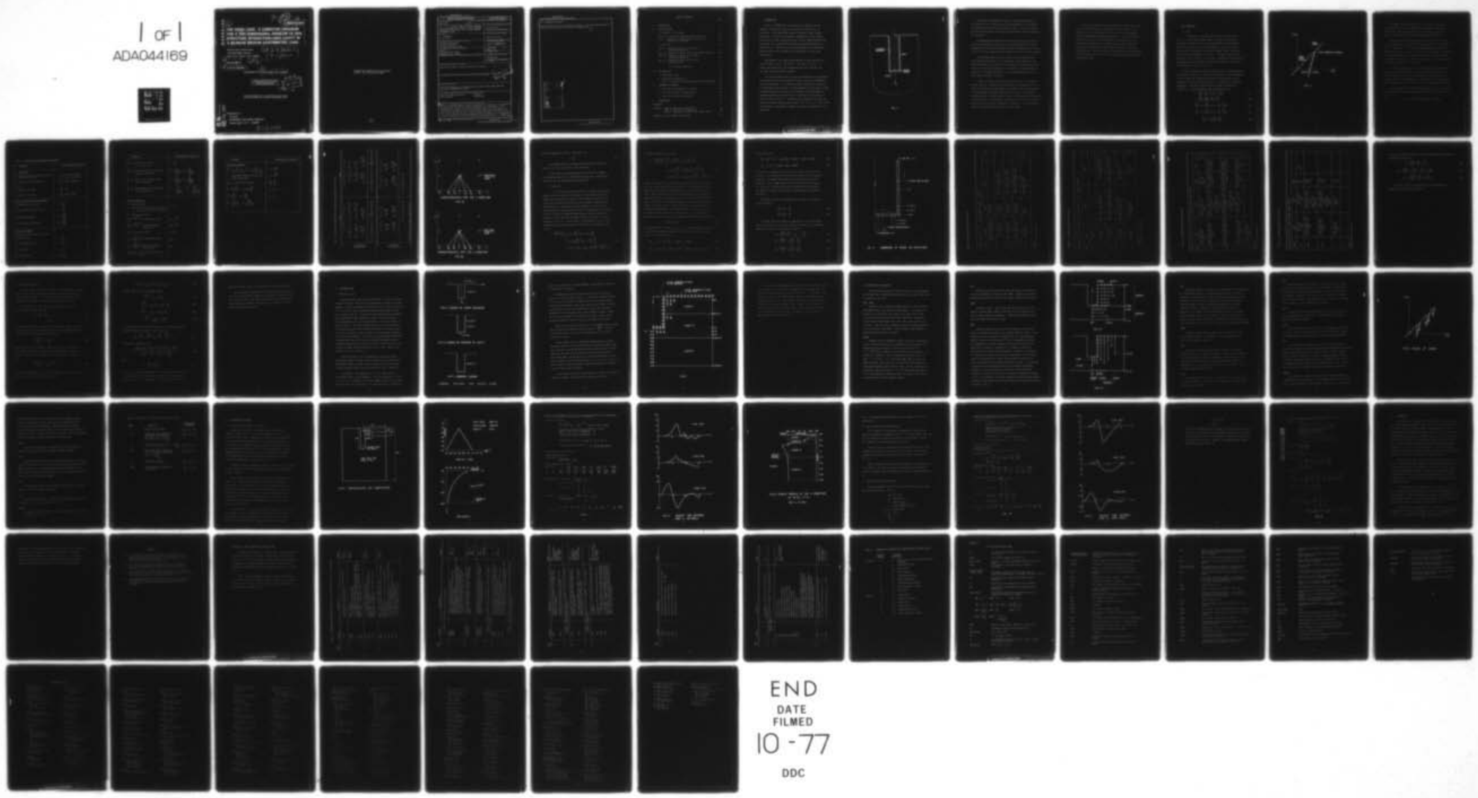

END

DATE

FILMED

10-77

DDC

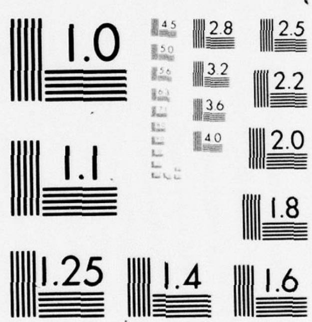

MICROCOPY RESOLUTION TEST CHART

NATIONAL BUREAU OF STANDARDS-1963-A

ADA044169

DNA 4299T

THE POSSI CODE - A COMPUTER PROGRAM FOR A TWO-DIMENSIONAL PROBLEM OF SOIL STRUCTURE INTERACTION-LINED CAVITY IN A BILINEAR MEDIUM AXISYMMETRIC CASE.

Weidlinger Associates
110 East 59th Street
New York, New York 10022

A. T. Matthews
H. H. Bleich

March 1977

67p.

Topical Report

CONTRACT No. DNA 001-76-C-0125

APPROVED FOR PUBLIC RELEASE;
DISTRIBUTION UNLIMITED.

THIS WORK SPONSORED BY THE DEFENSE NUCLEAR AGENCY
UNDER RDT&E RMSS CODE B344076464 Y99QAXSC06202 H2590D.

Prepared for
Director
DEFENSE NUCLEAR AGENCY
Washington, D. C. 20305

373 050

Destroy this report when it is no longer needed. Do not return to sender.

UNCLASSIFIED
SECURITY CLASSIFICATION OF THIS PAGE (When Data Entered)

REPORT DOCUMENTATION PAGE		READ INSTRUCTIONS BEFORE COMPLETING FORM
1. REPORT NUMBER DNA 4299T	2. GOVT ACCESSION NO.	3. RECIPIENT'S CATALOG NUMBER
4. TITLE (and Subtitle) A POSSI CODE—A COMPUTER PROGRAM FOR A TWO-DIMENSIONAL PROBLEM OF SOIL STRUCTURE INTERACTION-LINED CAVITY IN A BILINEAR MEDIUM AXISYMMETRIC CASE		5. TYPE OF REPORT & PERIOD COVERED Topical Report 6. PERFORMING ORG. REPORT NUMBER
7. AUTHOR(s) A. T. Matthews H. H. Bleich		8. CONTRACT OR GRANT NUMBER(s) DNA 001-76-C-0125
9. PERFORMING ORGANIZATION NAME AND ADDRESS Weidlinger Associates 110 East 59th Street New York, New York 10022		10. PROGRAM ELEMENT, PROJECT, TASK AREA & WORK UNIT NUMBERS Subtask Y99QAXSC062-02
11. CONTROLLING OFFICE NAME AND ADDRESS Director Defense Nuclear Agency Washington, D.C. 20305		12. REPORT DATE March 1977 13. NUMBER OF PAGES 78
14. MONITORING AGENCY NAME & ADDRESS(if different from Controlling Office)		15. SECURITY CLASS (of this report) UNCLASSIFIED 15a. DECLASSIFICATION/DOWNGRADING SCHEDULE

16. DISTRIBUTION STATEMENT (of this Report)

Approved for public release; distribution unlimited.

17. DISTRIBUTION STATEMENT (of the abstract entered in Block 20, if different from Report)

18. SUPPLEMENTARY NOTES

This work sponsored by the Defense Nuclear Agency under RDT&E RMSS Code B344076464 Y99QAXSC06202 H2590D.

19. KEY WORDS (Continue on reverse side if necessary and identify by block number)

Structure-Medium Interaction	Bilinear
Shell Response	Ground Shock

20. ABSTRACT (Continue on reverse side if necessary and identify by block number)

POSSI is a FORTRAN Computer code for computing the response of an axisymmetric soil/structure interaction problem cylindrical (r,z) coordinates. The configuration consists of a lined cylindrical cavity of finite length extending from the surface into a semi-infinite half-space, and loaded internally with a pressure p(z, T) or p(r, T) where applicable. The cavity lining is a thin cylindrical shell with bending stiffness, welded to an axisymmetric circular bottom plate with both bending and extensional motion. A right angle

next page

DD FORM 1 JAN 73 1473 EDITION OF 1 NOV 65 IS OBSOLETE

UNCLASSIFIED
SECURITY CLASSIFICATION OF THIS PAGE (When Data Entered)

20. ABSTRACT (Continued)

cont.
may be maintained at the plate/shell connection. The surrounding material is bilinear, with hysteresis in volumetric response only.

TABLE OF CONTENTS

I INTRODUCTION

POSSI is a FORTRAN code for computing the response of an axisymmetric soil/structure interaction problem in cylindrical (r, z) coordinates. The acronym POSSI stands for Problem of Soil Structure Interaction. The basic two dimensional configuration of the problem, consisting of a lined cylindrical cavity of finite length extending from the surface into a semi-infinite half-space and loaded internally, is shown in Fig. 1. Modification of certain parameters in the program do, however, permit use of the code for one dimensional, or free field calculations.

Development of the computational approach for POSSI has been presented in Refs. [1]-[4]. This report is the final one in that series, and presents not only information about use of the code, but also adds certain theoretical features.

The structure which lines the cavity is considered as an axisymmetric thin cylindrical shell with bending stiffness, welded to an axisymmetric circular bottom plate. In the previous reports the plate was considered to have bending stiffness only. The work presented in this report includes extensional motion of the plate. Also presented is the development of equations governing the maintenance of a right angle at the joining of plate and shell, see Fig. 1. In addition to the equations for these new features the basic equations given in Refs. [3], [4] have been repeated here for convenience, and grouped according to the order of computation in the POSSI code.

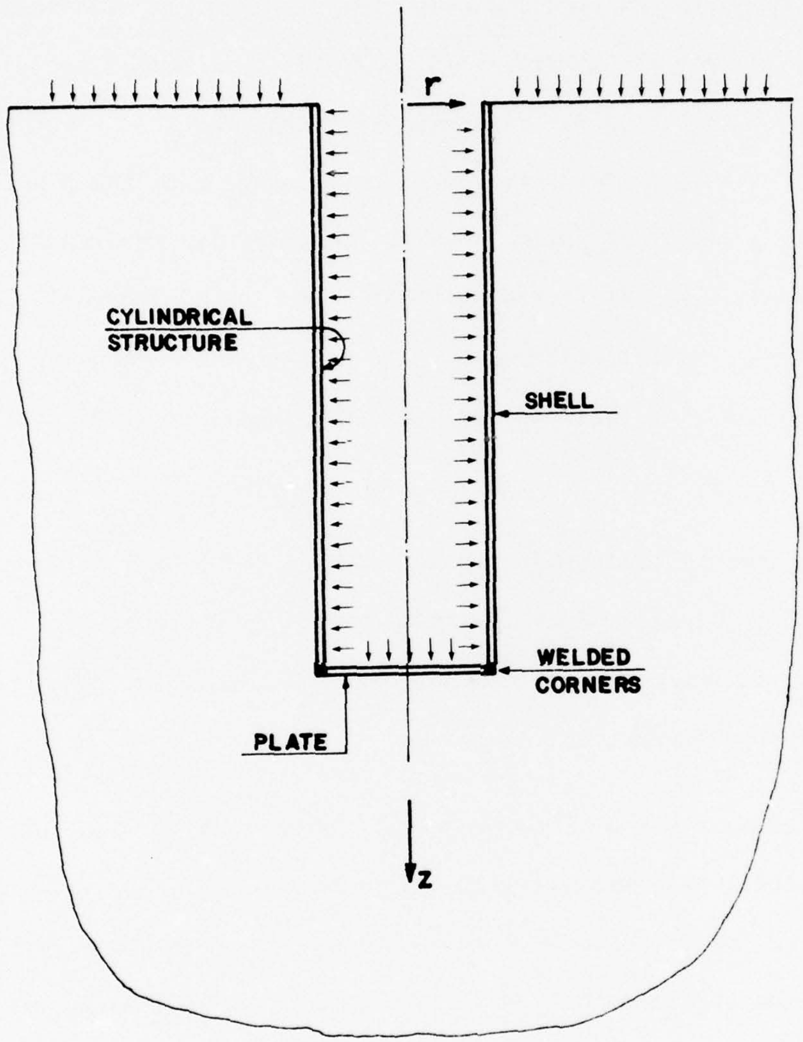

FIG. 1

The material surrounding the structure, and interacting with it, is considered to be a bilinear material, with hysteresis in the response of volumetric effects, but linear response in shear. Provision is made for horizontal layering of the material, with different material properties for each layer.

The computational scheme used to describe the response of points in the field surrounding the structure is the pseudo-characteristic scheme combined with a fractional step method that was developed in Refs. [1]-[4]. As in Ref. [3] this scheme will be hereinafter referred to as the PC scheme.

The governing equations for the motion of the structural lining were obtained from a method of the variational calculus applied to the finite difference form of the total strain energy. The right-angle condition at the joining was introduced as an equation of constraint with the addition of a Lagrangian multiplier. The resulting equations are first order finite-difference in nature.

A number of options are built into the POSSI code. They include: location and type of applied load; dimensional or non-dimensional output; lined or unlined cavity; right-angle at plate-shell connection maintained or not maintained; horizontal layering in the field, or no horizontal layering; graphic or printed output, or both; one-dimensional configurations in either r-t or z-t coordinates as special cases; the shell and the plate may have different material properties or thicknesses. These, and other features, are discussed in Section III of this report.

In order to illustrate use of the POSS1 code typical output from three sets of computations are presented. The first case is for an unlined cavity in a layered material, subjected to a time dependent, and location dependent internal pressure p(z, t). Two one-dimensional subcases are also very briefly discussed. The second case is for a structurally lined cavity, in a layered material with a right angle maintained at the shell-plate connection, subjected to an internal pressure p(z, t). Results in this case are presented in non-dimensional form. The third case is a rerun of the second, with results presented in dimensional form.

II BASIC EQUATIONS

A. Field

The material surrounding the structure acts linearly in shear (i.e. G, the shear modulus, remains constant), but bilinearly in volumetric response. That is, the bulk modulus K has two possible values: $K = K_{LD}$ for $(-J_1)$ in virgin loading, $K = K_{UN}$ for $(-J_1)$ less than or equal to the previous compressive maximum. Figure 2 shows how this restricts the dependency of ε_v on J_1. The model continues onto the tensile side of the J_1, ε_v curve along a straight line of essentially unloading slope, unless tension is experienced initially, in which case the loading slope is used. See Fig. 2.

The basic differential equations which describe the material motion are the same as those for a linear elastic continuum. Only the parameters K (bulk modulus) and ν (Poisson ratio) must be appropriately chosen, according to the criteria mentioned above, for conditions of loading or unloading. G (the shear modulus) remains constant throughout the computation. In non-dimensional terms these equations are

$$\mu \frac{\partial V_r}{\partial \tau} = \frac{\partial \sigma_r}{\partial r} + \frac{\sigma_r - \sigma_\theta}{r} + \frac{\partial \sigma_{rz}}{\partial z} \tag{1}$$

$$\mu \frac{\partial V_z}{\partial \tau} = \frac{\partial \sigma_{rz}}{\partial r} + \frac{\sigma_{rz}}{r} + \frac{\partial \sigma_z}{\partial z} \tag{2}$$

$$\frac{\partial \sigma_r}{\partial \tau} = \mu\lambda^2 \left[\frac{\partial V_r}{\partial r} + \frac{\nu}{1 - \nu} \left(\frac{V_r}{r} + \frac{\partial V_z}{\partial z}\right)\right] \tag{3}$$

$$\frac{\partial \sigma_z}{\partial \tau} = \mu\lambda^2 \left[\frac{\partial V_z}{\partial z} + \frac{\nu}{1 - \nu} \left(\frac{V_r}{r} + \frac{\partial V_z}{\partial r}\right)\right] \tag{4}$$

$$\frac{\partial \sigma_{rz}}{\partial \tau} = \mu\lambda_s^2 \left[\frac{\partial V_z}{\partial r} + \frac{\partial V_r}{\partial z}\right] \tag{5}$$

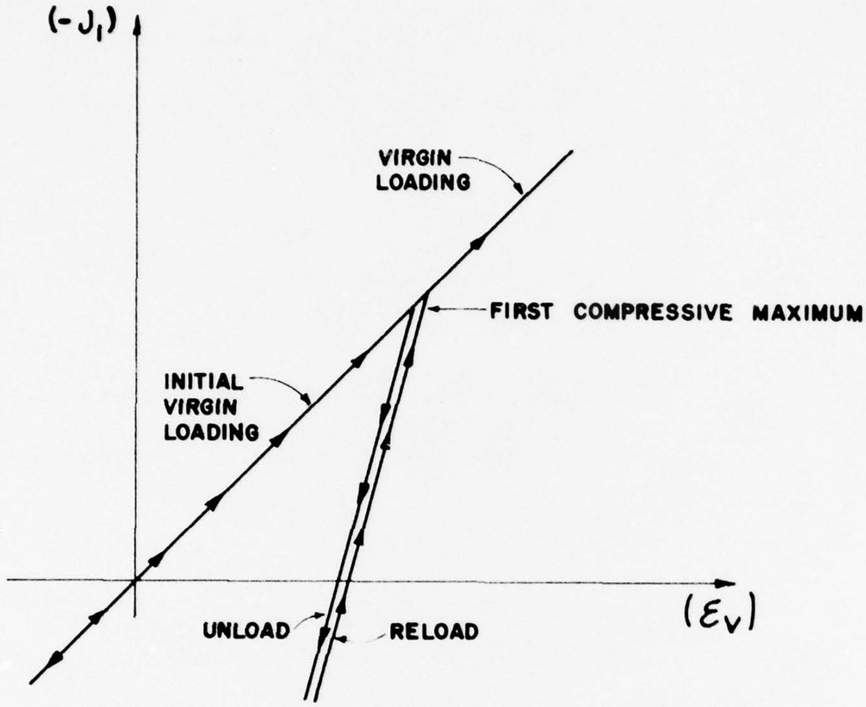

(- J1)
VIRGIN LOADING
FIRST COMPRESSIVE MAXIMUM
INITIAL VIRGIN LOADING
UNLOAD
RELOAD
(εv)

FIG. 2

The symbols are defined in Table 1, as are all the parameters, the stresses, velocities and displacements which appear in the basic equations for both field and structure. The quantities appearing in Table 1 are given in both dimensional and non-dimensional form.

Using the method of fractional steps the basic equations, with r, z and t dependencies are separated into two problems: in r, t coordinates; in z, t coordinates. Each is then a one-dimensional wave propagation problem with its own set of P-, S- and "zero"-characteristics. Integration is set up along these characteristics resulting in the equations which are summarized in Table 2. (The superscripts refer to points in the space time meshes, shown in Figs. 3a and 3b.)

In order to obtain values of stress and velocity at points intermediate to the mesh points (i.e. at the R and Q pts. shown in Figs. 3a and 3b, between L-1, L and L, L+1, respectively) a three point interpolation scheme was used leading to a "second order" integration scheme which exhibits errors of Δr^2 and Δz^2 in r- and z-directions respectively.

As an example of this interpolation scheme, if F_{R_P}, is the value of the quantity to be found from known quantities F_L, F_{L-1}, F_{L+1} (Fig. 3a) then

$$F_{R_P} = (1-\alpha^2)F_L + \frac{\alpha}{2}(\alpha-1)F_{L+1} + \frac{\alpha}{2}(\alpha+1)F_L-1 \qquad (6)$$

TABLE I PARAMETERS AND NON-DIMENSIONAL PARAMETERS

	PARAMETERS	NON-DIMENSIONAL PARAMETERS
1.	COORDINATES	
	R_0 Reference radius. Usually the nominal radius of the cavity	$r = \frac{R}{R_0}$ radial coordinate, r_{LC} = cavity radius
	R, Z Radial and depth coordinates	$z = \frac{Z}{R_0}$ depth coordinate
	t Time	
	C Reference wave speed	$\tau = \frac{Ct}{R_0}$ time
	L Length of the cavity	$\ell = \frac{L}{R_0}$ cavity length
2.	PARTICLE VELOCITIES AND DISPLACEMENTS	
	$\dot{U}_r$ Radial particle velocity	$V_r = \frac{\rho C \dot{U}_r}{p_0}$
	$\dot{U}_z$ Longitudinal particle velocity	$V_z = \frac{\rho C \dot{U}_z}{p_0}$
	U_r Radial displacement	$W_r = \frac{\rho C^2 U_r}{R_0 p_0}$
	U_z Longitudinal displacement	$W_z = \frac{\rho C^2 U_z}{R_0 p_0}$
3.	FORCES AND STRESSES	
	p_0 Reference stress from applied load	
	$\bar{\sigma}_r$ Radial stress	$\sigma_r = \frac{\bar{\sigma}_r}{p_0}$
	$\bar{\sigma}_z$ Longitudinal stress	$\sigma_z = \frac{\bar{\sigma}_z}{p_0}$
	$\bar{\sigma}_\theta$ Hoop stress	$\sigma_\theta = \frac{\bar{\sigma}_\theta}{p_0}$
	$\bar{\sigma}_{rz}$ Shear stress	$\sigma_{rz} = \frac{\bar{\sigma}_{rz}}{p_0}$

	PARAMETERS	NON-DIMENSIONAL PARAMETERS
4.	$\bar{J}_1$ First invariant of stress $\bar{J}_1 = \bar{\sigma}_r + \bar{\sigma}_z + \bar{\sigma}_\theta$	$J_1 = \dfrac{\bar{J}_1}{p_0}$
	$\bar{N}_s$, $\bar{N}_p$ Longitudinal forces in the shell and plate, respectively	$N_s = \dfrac{\bar{N}_s}{\left(\dfrac{p_0 D_s R_0}{\rho C^2}\right)}$, $N_p = \dfrac{\bar{N}_p}{\left(\dfrac{p_0 D_p R_0}{\rho C^2}\right)}$
	$\bar{Q}_s$, $\bar{Q}_p$ Shear forces in the shell and plate, respectively	$Q_s = \dfrac{\bar{Q}_s}{\left(\dfrac{p_0 D_s R_0}{\rho C^2}\right)}$, $Q_p = \dfrac{\bar{Q}_p}{\left(\dfrac{p_0 D_p R_0}{\rho C^2}\right)}$
	$\bar{M}_s$, $\bar{M}_p$ Bending moments in the shell and plate, respectively	$M_s = \dfrac{\bar{M}_s}{\left(\dfrac{p_0 D_s}{\rho C^2}\right) R_0^2}$, $M_p = \dfrac{\bar{M}_p}{\left(\dfrac{p_0 D_p}{\rho C^2}\right) R_0^2}$
5.	<u>MATERIAL PROPERTIES</u>	
	ρ Reference density	
	ρ_i Material density of field (a different ρ_i will be specified for each layer)	$\mu = \dfrac{\rho_i}{\rho}$
	C Reference wave speed	
	$C_{LD}^2 = \dfrac{K_{LD} + \frac{4}{3} G}{\rho}$ Loading P-wave speed	$\lambda_{LD} = \dfrac{C_{LD}}{C}$
	$C_{UN}^2 = \dfrac{K_{UN} + \frac{4}{3} G}{\rho}$ Unloading-Reloading P-wave speed	$\lambda_{UN} = \dfrac{C_{UN}}{C}$
	$C_s^2 = \dfrac{G}{\rho}$ Shear wave speed	$\lambda_s = \dfrac{C_s}{C}$
	$\nu_{LD} = \dfrac{3K_{LD} - 2G}{6K_{LD} + 2G}$ Loading Poisson ratio	ν_{LD}
	$\nu_{UN} = \dfrac{3K_{UN} - 2G}{6K_{UN} + 2G}$ Unloading-Reloading Poisson ratio	ν_{UN}
	C_{LD}, C_{UN}, C_s will be specified for each layer	

PARAMETERS	NON-DIMENSIONAL PARAMETERS
6. STRUCTURE PROPERTIES	
$\Omega_s^2 = \frac{E_s}{(1-\nu_s^2)\,\rho_s\,R_0^2}$, $\Omega_p^2 = \frac{E_p}{(1-\nu_p^2)\,\rho_p\,R_0^2}$	$\omega_s = \frac{\Omega_s R_0}{C}$
Fundamental frequency for shell and plate, respectively	$\omega_p = \frac{\Omega_p R_0}{C}$
h_s, h_p Shell, plate thickness	$\frac{h_s}{R_0}$, $\frac{h_p}{R_0}$
$\alpha_s = \frac{1}{12}\left(\frac{h_s}{R_0}\right)^2$, $\alpha_p = \frac{1}{12}\left(\frac{h_p}{R_0}\right)^2$	α_s , α_p
$\beta_s = \frac{\rho R_0}{\rho_s h_s}$, $\beta_p = \frac{\rho R_0}{\rho_p h_p}$	β_s , β_p
$D_s = \frac{E_s h_s}{R_0(1-\nu_s^2)}$, $D_p = \frac{E_p h_p}{R_0(1-\nu_p^2)}$	

TABLE 2 EQUATIONS FOR COMPUTATION OF STRESSES AND VELOCITIES IN THE FIELD

	P-waves	S-waves
SUBROUTINE RDIR R-DIRECTION	$P_p = \sigma_r + \lambda V_r \quad , \quad M_p = \sigma_r - \lambda V_r$	$P_s = \sigma_{rz} + \lambda_s V_z \qquad M_s = \sigma_{rz} - \lambda_s V_z$
	$P_p^N = \frac{\lambda\Delta\tau}{r^N + \lambda\Delta\tau} [\sigma_r - \sigma_\theta + \frac{\nu}{1-\nu} \lambda V_r]^{Q_p} + P_p^{Q_p}$	$P_s^N = \frac{\lambda_s \Delta\tau}{r^N + \lambda_s \Delta\tau} \sigma_{rz}^{Q_s} + P_s^{Q_s}$
	$M_p^N = - \frac{\lambda\Delta\tau}{r^N + \lambda\Delta\tau} [\sigma_r - \sigma_\theta - \frac{\nu}{1-\nu} \lambda V_r]^{R_p} + M_p^{R_p}$	$M_s^N = \frac{\lambda_s \Delta\tau}{r^N + \lambda_s \Delta\tau} \sigma_{rz}^{R_s} + M_s^{R_s}$
	$\sigma_r^N = \frac{P_p^N + M_p^N}{2} \qquad V_r^N = \frac{P_p^N - M_p^N}{2\lambda}$	$\sigma_{rz}^N = \frac{P_s^N + M_s^M}{2} \qquad V_z^N = \frac{P_s^N - M_s^N}{2\lambda_s}$
	$\sigma_z^N = \sigma_z^L + \frac{\nu}{1-\nu}(\sigma_r^N - \sigma_r^L) + \lambda^2 \Delta\tau \frac{V_r^N}{r^N} (\frac{\nu}{1-\nu}) (\frac{1-2\nu}{1-\nu})$	$J_1^N = J_1^L + \frac{1+\nu}{1-\nu} (\sigma_r^N - \sigma_r^L) + \lambda^2 \Delta\tau \frac{V_r^N}{r^N} (\frac{1+\nu}{1-\nu}) (\frac{1-2\nu}{1-\nu})$
SUBROUTINE ZDIR Z-DIRECTION	$\bar{P}_p = \sigma_z + \lambda V_z \qquad \bar{M}_p = \sigma_z - \lambda V_z$	$\bar{P}_s = \sigma_{rz} + \lambda V_r \qquad \bar{M}_s = \sigma_{rz} - \lambda V_z$
	$\bar{P}_p^N = \bar{P}_p^{\bar{Q}_p} \qquad \bar{M}_p^N = \bar{M}_p^{\bar{R}_p}$	$\bar{P}_s^N = \bar{P}_s^{\bar{Q}_s} \qquad \bar{M}_s^N = \bar{M}_s^{\bar{R}_s}$
	$\sigma_z^N = \frac{\bar{P}_p^N + \bar{M}_p^N}{2} \qquad V_z^N = \frac{\bar{P}_p^N - \bar{M}_p^N}{2\lambda}$	$\sigma_{rz}^N = \frac{\bar{P}_s^N + \bar{M}_s^N}{2} \qquad V_r^N = \frac{\bar{P}_s^N - \bar{M}_s^N}{2\lambda_s}$
	$\sigma_r^N = \sigma_r^L + \frac{\nu}{1-\nu} (\sigma_z^N - \sigma_z^L)$	$J_1^N = J_1^L + \frac{1+\nu}{1-\nu} (\sigma_z^N - \sigma_z^L)$
	Superscripts refer to points in Figs. 3a and 3b	

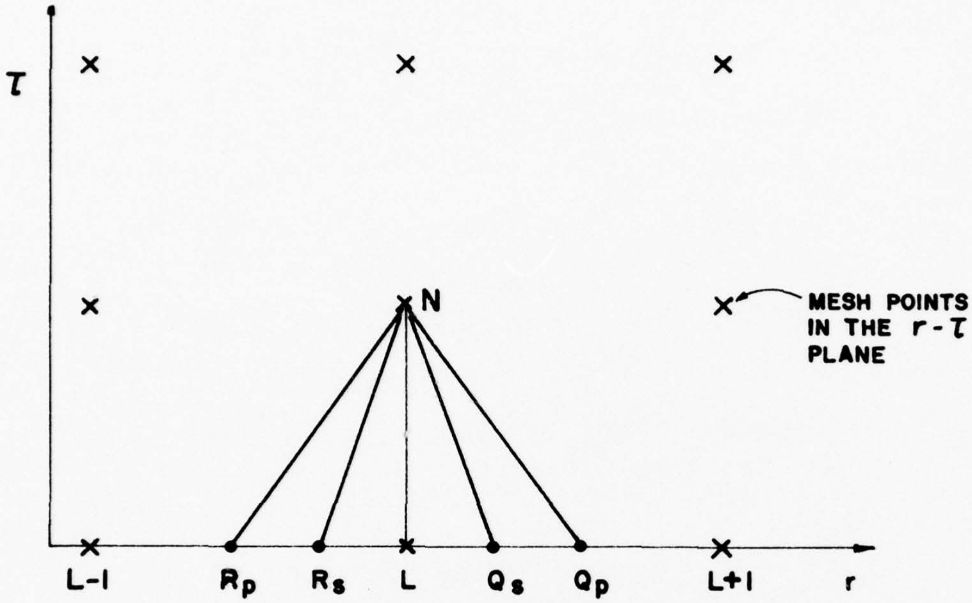

CHARACTERISTICS FOR THE r-DIRECTION

FIG. 3a

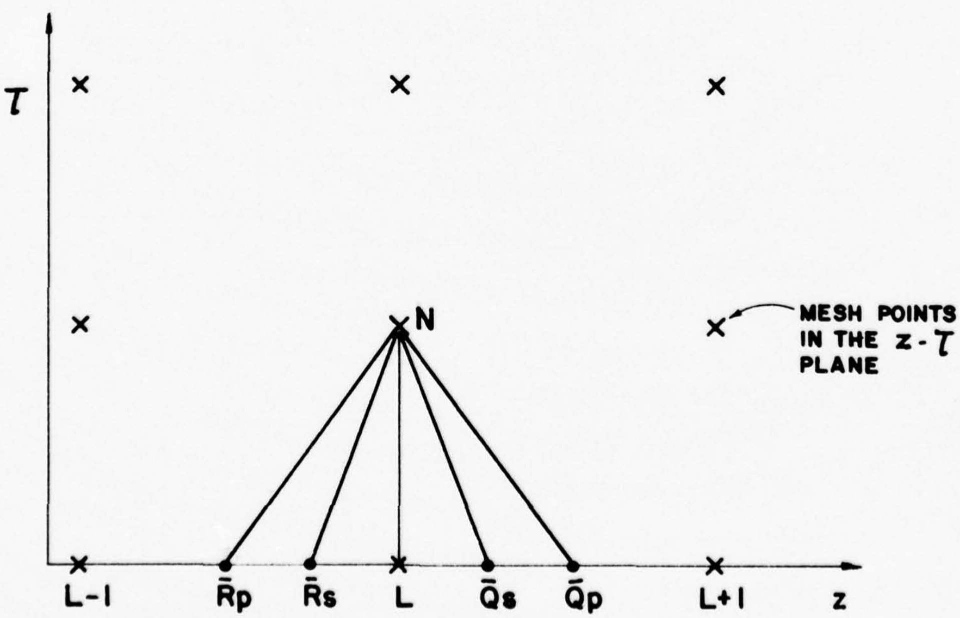

CHARACTERISTICS FOR THE z-DIRECTION

FIG. 3b

where the appropriate value of λ determines α as

$$\alpha = \frac{\lambda \Delta \tau}{\Delta r} \tag{7}$$

In the POSSI Code this interpolation scheme has been used at all points in the field in both the r- and z-directions.

The PC-scheme as outlined above does not provide for following or maintaining shock fronts. Computational results from a loading with a very short rise time would therefore be dispersed.

B. Structure

The structure lining the cavity is a cylindrical shell with bending stiffness, welded at the bottom to a flat circular plate which deforms both by bending and extension. The equations of motion in both radial and longitudinal directions for both structural components have been obtained by a variational procedure applied to the total strain energy expressed in finite difference form. The expressions for potential energy of the shell (including bending energy, extensional energy and work done by the loads) plus the kinetic energy of the shell are given in Appendix B of Ref. [4]. Repeated here, for convenience, in terms of the non-dimensional quantities defined in Table 1, the total energy for the shell is

$$\begin{aligned} U_s = \frac{\pi D_s R_0}{\omega_s^2} \left(\frac{R_0}{C^2}\right) \int_0^{\ell} \Big\{ & \frac{1}{2} \omega_s^2 \left[\left(\frac{\partial W_z}{\partial z}\right)^2 + W_r^2 + 2\nu_s W_r \frac{\partial W_z}{\partial z} \right] \\ & + \frac{1}{2} \alpha_s \omega_s^2 \left[\left(\frac{\partial^2 W_r}{\partial z^2}\right)^2 + W_r^2 - 2 \frac{\partial W_z}{\partial z} \frac{\partial^2 W_r}{\partial z^2} \right] \\ & - \beta_s \left[(p + \sigma_r) W_r + \sigma_{rz} W_z \right] + \frac{1}{2} \left[\left(\frac{\partial W_r}{\partial \tau}\right)^2 + \left(\frac{\partial W_z}{\partial \tau}\right)^2 \right] \Big\} \, dz \end{aligned} \tag{8}$$

A similar expression for the plate

$$U_p = \frac{\pi D_s R_0}{\omega_s^2}\left(\frac{R_0}{\rho C^2}\right)^2 \int_0^{r_{LC}} \left\{ \frac{1}{2}\omega_p^2 \left[\left(\frac{\partial W_r}{\partial r}\right)^2 + 2\nu_p \frac{W_r}{r}\frac{\partial W_r}{\partial r} + \frac{W_r^2}{r^2} + \right. \right.$$

$$+ \frac{1}{2}\alpha_p \omega_p^2 \left[\left(\frac{\partial^2 W_z}{\partial r^2}\right)^2 + \frac{1}{r^2}\left(\frac{\partial W_z}{\partial r}\right)^2 + \frac{2\nu_p}{r}\frac{\partial^2 W_z}{\partial r^2}\frac{\partial W_z}{\partial r}\right] \tag{9}$$

$$\left. -\beta_p\left[(p + \sigma_z)W_z + \sigma_{rz}W_r\right] + \frac{1}{2}\left[\left(\frac{\partial^2 W_r}{\partial \tau^2}\right) + \left(\frac{\partial^2 W_z}{\partial \tau^2}\right)\right]\right\} r\, dr$$

includes the energy of extensional plate motion which was excluded from the plate energy expression given in Ref. [4]. The derivatives in these expressions are written in finite-difference form at every point on the shell. Central differences are used for non-boundary points, forward or backward differences, as appropriate, are used for points in the neighborhood of the corner. A variational procedure is then applied to the total energy, first with respect to radial displacement, then with respect to longitudinal displacement. See Appendix B, Ref. [4]. The result is two equations of motion, one in the r-direction, one in the z-direction at each point of the structure. These equations may be written symbolically as

$$V_m^N = V_m^L + A_m^L \Delta\tau \tag{10}$$

The subscript "m" is written as r_s, z_s, r_p, z_p depending upon the direction of motion being computed, and whether the term comes from shell or plate effects. The quantities A_m^L are

$$A_{z_s}^L = \beta_s \sigma_{rz}^L + \omega_s^2[D2ZWZ + \nu_s\ D1ZWR + \alpha_s\ D3ZWR] \tag{11}$$

$$A_{r_s}^L = \beta_s(p^L + \sigma_r^L) - \omega_s^2[(1 + \alpha_s)W_r^L + \nu_s\ D1ZWZ + \alpha_s(D4ZWR - D3ZWZ)] \tag{12}$$

for the shell, and

$$A^L_{z_p} = \beta_p(p^L + \sigma^L_z) - \alpha_p\omega^2_p\ [D4RWZ + 2(D3RWZ) - D2RWZ + D1RWZ] \tag{13}$$

$$A^L_{r_p} = \beta_p\sigma^L_{rz} + \omega^2_p\ [D2RWR + D1RWR + D0RWR] \tag{14}$$

for the plate. The superscript "L" refers to a point on the structure, see Fig. 4. The superscript "N" refers to the new value of the quantity at point L. The symbol D2RWZ stands for the second derivative with respect to r of W_z, D1ZWR stands for the first derivative with respect to z of W_r, etc. The finite difference expressions for these symbols are tabulated in Table 3a and 3b (for the shell), Tables 4a and 4b (for the plate).

Equations (10)-(14) are expressions for velocities. The displacements are found as

$$W^N_z = W^L_z + \Delta\tau V^N_z \tag{15}$$

$$W^N_r = W^L_r + \Delta\tau V^N_r \tag{16}$$

The POSSI code also provides for computation of forces and moments within the structure. For the shell portion the normal, shear and moment quantities per unit of circumferential length are

$$\bar{N}_s = \frac{p_0 D_s R_0}{\rho C^2} \left[\frac{\partial W_z}{\partial z} + \nu_s W_r - \alpha_s \frac{\partial^2 W_r}{\partial z^2}\right] \tag{17}$$

$$\bar{Q}_s = \frac{p_0 D_s R_0}{\rho C^2}\ \alpha_s\left[\frac{\partial^3 W_r}{\partial z^3} - \frac{\partial^2 W_z}{\partial z^2}\right] \tag{18}$$

$$\bar{M}_s = \frac{p_0 D_s R_0}{\rho C^2}\ \alpha_s\left[\frac{\partial^3 W_r}{\partial z^2} - \frac{\partial^2 W_r}{\partial z^2}\right] \tag{19}$$

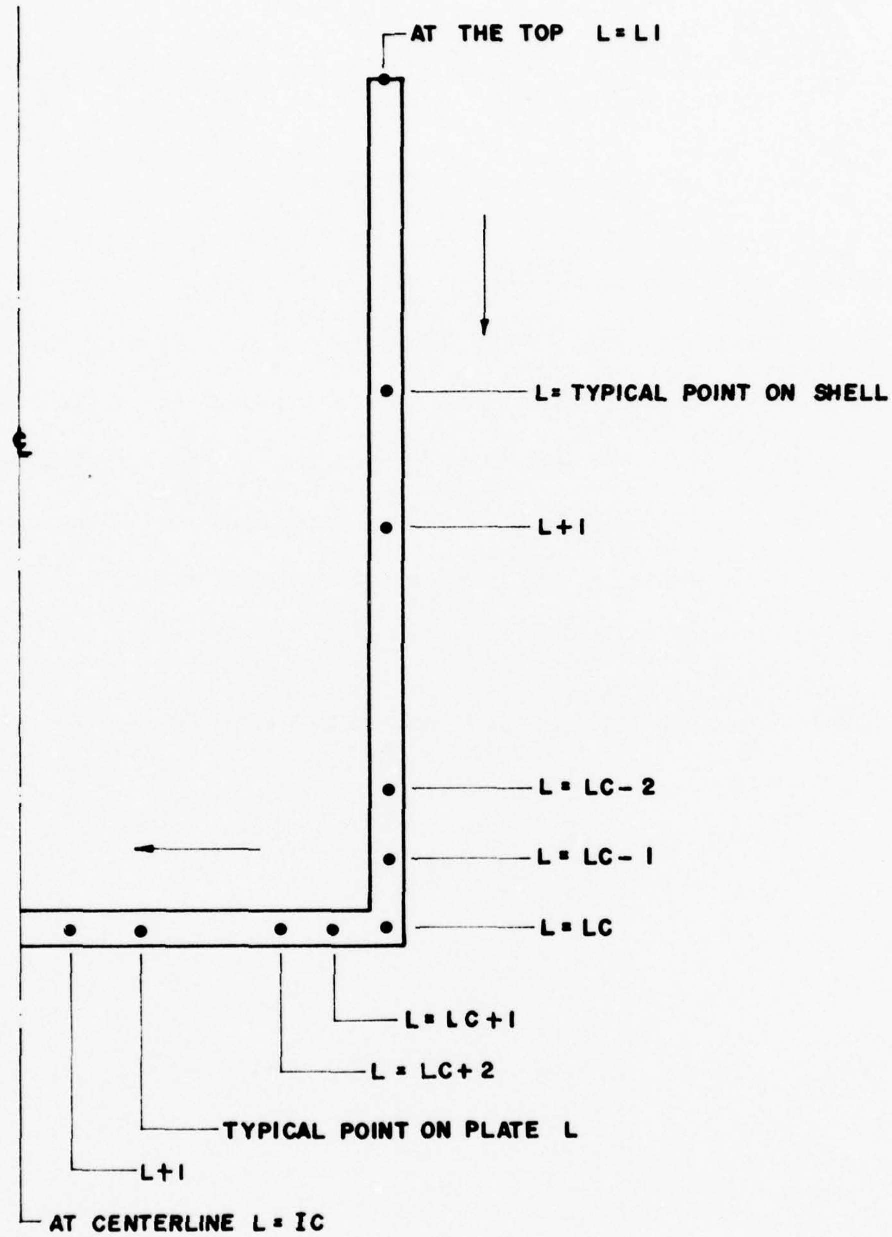

FIG. 4 NUMBERING OF POINTS ON STRUCTURE

TABLE 3a EQUATIONS OF MOTION FOR THE SHELL

Longitudinal Motion: $V_z^N = V_z^L + \Delta\tau \{\beta_s \sigma_{rz}^L + \omega_s^2 [D2ZWZ + \nu_s D1ZWR - \alpha_s D3ZWR]\} \bar{c}$

Points*	D2ZWZ	D1ZWR	D3ZWR	$\bar{c}$
L=L1	$\left[\frac{W_z^{L1+2} - 2W_z^{L1+1} + W_z^{L1}}{\Delta z^2}\right](1-\alpha_s)$	$\frac{W_r^{L1+1} - W_r^{L1}}{\Delta z}$	0	1
L	$\frac{W_z^{L+1} - 2W_z^{L} + W_z^{L-1}}{\Delta z^2}$	$(\frac{W_r^{L+1} - W_r^{L-1}}{2\Delta z})$	$(\frac{W_r^{L+2} - 2W_r^{L+1} + 2W_r^{L-1} - W_r^{L-2}}{2\Delta z^3})$	1
L=LC-2	$\frac{W_z^{LC-1} - 2W_z^{LC-2} + W_z^{LC-3}}{\Delta z^2}$	$(\frac{W_r^{LC-1} - W_r^{LC-2}}{\Delta z})$	$(\frac{W_r^{LC} - 3W_r^{LC-2} + 3W_r^{LC-3} - W_r^{LC-4}}{\Delta z^3})$	1
L=LC-1	$\frac{.5W_z^{LC} - 1.5W_z^{LC-1} + W_z^{LC-2}}{\Delta z^2}$	$(\frac{.5W_r^{LC} - W_r^{LC-1}}{\Delta z})$	$\frac{.5W_r^{LC} - 2W_r^{LC-1} + 2.5W_r^{LC-2} - W_r^{LC-3}}{\Delta z^3}$	1
L=LC	$(\frac{W_z^{LC-1} - W_z^{LC}}{\Delta z^2})$	$(\frac{-W_r^{LC}}{\Delta z})$	$(\frac{-W_r^{LC} + 2W_r^{LC-1} - W_r^{LC-2}}{\Delta z^3})$	$\frac{1}{1+\gamma}$ **

* See Fig. 4

** See Eq. (27) for definition of γ

TABLE 3b EQUATIONS OF MOTION FOR THE SHELL

Radial Motion: $V_r^N = V_r^L + \Delta\tau \{\beta_s(p^L + \sigma_r^L) - \omega_s^2[(1 + \alpha_s)W_r^L + \nu_s \, D1ZWZ + \alpha_s(D4ZWR + D3ZWZ)]\}\,\bar{c}$

Points*	D1ZWZ	D4ZWR	D3ZWZ	$\bar{c}$
L=1	$\frac{-\nu_s}{1-\alpha_s} W_r^{L1}$	0	0	1.
L	$\frac{W_z^{L+1} - W_z^{L-1}}{2\Delta z}$	$\frac{W_r^{L+2} - 4W_r^{L+1} + 6W_r^{L} - 4W_r^{L-1} + W_r^{L-2}}{\Delta z^4}$	$\frac{W_z^{L-2} - 2W_z^{L-1} + 2W_z^{L+1} + W_z^{L+2}}{2\Delta z^3}$	1.
L=LC-2	$\frac{W_z^{LC-2} - W_z^{LC-3}}{\Delta z}$	$\frac{.5W_r^{LC} - 3W_r^{LC-1} + 5.5W_r^{LC-2} - 4W_r^{LC-3} + W_r^{LC-4}}{\Delta z^4}$	$\frac{-.5W_z^{LC} + 2.5W^{LC-1} - 3W_z^{LC-2} + W_z^{LC-3}}{\Delta z^3}$	1.
L=LC-1	$\frac{W_z^{LC-1} - W_z^{LC-2}}{\Delta z}$	$\frac{-W_r^{LC} + 3W_r^{LC-1} - 3W_r^{LC-2} + W_r^{LC-3}}{\Delta z^4}$	$\frac{W_z^{LC} - 2W_z^{LC-1} + W_z^{LC-2}}{\Delta z^3}$	1.
L=LC	$\frac{W_z^{LC} - W_z^{LC-1}}{\Delta z}$	$\frac{W_r^{LC} - 2W_r^{LC-1} + W_r^{LC-2}}{\Delta z^4}$	$\frac{W_z^{LC-1} - W_z^{LC}}{\Delta z^3}$	$\frac{1}{1+\gamma}$**

*See Fig. 4

** See Eq. (27) for definition of γ

TABLE 4a EQUATIONS OF MOTION FOR THE PLATE

Longitudinal Motion: $V_z^N = V_z^L + \Delta\tau\{\beta_p(\sigma_z + p)^L - \omega_p^2\alpha_p[\mathrm{D4RWZ} + \mathrm{D3RWZ} - \mathrm{D2RWZ} + \mathrm{D1RWZ}]\}\,\bar{c}$					
Points*	D4RWZ	D3RWZ	D2RWZ	D1RWZ	$\bar{c}$
L=LC	$\frac{(W_z^{LC+2} - 2W_z^{LC+1} + W_z^{LC})}{(\Delta r)^4}$	$\nu_p \frac{(W_z^{LC+2} - 3.W_z^{LC+1} + 2.W_z^{LC})}{r_{LC}(\Delta r)^3}$	$\frac{W_z^{LC+1} - W_z^{LC}}{r_{LC}^2(\Delta r)^2}$	0	$\frac{\gamma}{1+\gamma}$ **
L=LC+1	$\frac{(W_z^{LC+3} - 3W_z^{LC+2} + 3W_z^{LC+1} - W_z^{LC})}{(\Delta r)^4}$	$\nu_p \frac{(W_z^{LC+3} - 3.5W_z^{LC+2} + 4.W_z^{LC+1} - 1.5W_z^{LC})}{r_{LC+1}(\Delta r)^3}$ $\frac{(-W_z^{LC+2} + 2W_z^{LC+1} - W_z^{LC})}{r_{LC+1}(\Delta r)^3}$	$\frac{W_z^{LC+2} - 1.5W_z^{LC+1} + .5W_z^{LC}}{r_{LC+1}r_{LC}(\Delta r)^2}$	$\frac{(-W_z^{LC+2} + W_z^{LC+1})}{(r_{LC+1})^2 r_{LC}\Delta r}$	1.
L=LC+2	$\frac{W_z^{LC+4} - 4W_z^{LC+3} + 5.5W_z^{LC+2} - 3W_z^{LC+1} + .5W_z^{LC}}{(\Delta r)^4}$	$\nu_p \frac{(W_z^{LC+4} - 4W_z^{LC+3} + 6W_z^{LC+2} - 3.5W_z^{LC+1} + .5W_z^{LC})}{r_{LC+2}(\Delta r)^3}$ $\frac{-2W_z^{LC+3} + 5W_z^{LC+2} - 2W_z^{LC+1} + W_z^{LC}}{r_{LC+2}(\Delta r)^3}$	$\frac{+W_z^{LC+3} - 2W_z^{LC+2} + W_z^{LC+1}}{r_{LC+2}r_{LC+1}(\Delta r)^2}$	$\frac{-W_z^{LC+3} + W_z^{LC+2}}{(r_{LC+2})^2 r_{LC+1}\Delta r}$	1.
L	$\frac{W_z^{L+2} - 4W_z^{L+1} + 6W_z^{L} - 4W_z^{L-1} + W_z^{L-2}}{(\Delta r)^4}$	$\frac{-W_z^{L+2} + 2W_z^{L+1} - 2W_z^{L-1} + W_z^{L-2}}{r_L\Delta r^3}$	$\frac{+W_z^{L+1} - 2W_z^{L} + W_z^{L-1}}{r_L^2(\Delta r)^2}$	$\frac{-.5W_z^{L+1} + .5W_z^{L-1}}{r_L^3\Delta r}$	1.
L=IC	$\frac{18W_z^{IC} - 24W_z^{IC-1} + 6W_z^{IC-2}}{(\Delta r)^4}$	0	0	0	1.

*See Fig. 4

** See Eq. (27) for definition of γ

TABLE 4b EQUATIONS OF MOTION FOR THE PLATE

Radial Motion: $V_r^N = V_r^L + \Delta\tau\{\beta_p \sigma_{rz}^L + \omega_p^2 [D2RWR + D1RWR - D0RWR]\}\,\bar{c}$

Points*	D2RWR	D1RWR	D0RWR	$\bar{c}$
L=LC	$\frac{W_r^{LC+1} - W_r^{LC}}{(\Delta r)^2}$	$\nu_p \frac{(W_r^{LC+1} - 2W_r^{LC})}{r_{LC}\Delta r}$	$-\frac{W_r^{LC}}{r_{LC}^2}$	$\frac{\gamma}{1+\gamma}$ **
L=LC+1	$\frac{W_r^{LC+2} - 1.5W_r^{LC+1} + .5W_r^{LC}}{(\Delta r)^2}$	$\nu_p \frac{(W_r^{LC+2} - 2W_r^{LC+1} + .5W_r^{LC})}{r_{LC+1}\Delta r} + \frac{-.5W_r^{LC+1} + .5W_r^{LC}}{r_{LC+1}\Delta r}$	$-\frac{W_r^{LC+1}}{r_{LC+1}^2}$	1
L=LC+2	$\frac{W_r^{LC+3} - 2W_r^{LC+2} + W_r^{LC+1}}{(\Delta r)^2}$	$\nu_p \frac{(W_r^{LC+3} - 2W_r^{LC+2} + W_r^{LC+1})}{r_{LC+2}\Delta r} + \frac{-W_r^{LC+2} + W_r^{LC+1}}{r_{LC+2}\Delta r}$	$-\frac{W_r^{LC+2}}{r_{LC+2}^2}$	1
L	$\frac{W_r^{L+1} - 2W_r^{L} + W_r^{L-1}}{(\Delta r)^2}$	$\frac{-W_r^{L+1} + W_r^{L}}{2r_L\Delta r}$	$-\frac{W_r^{L}}{r_L^2}$	1
L=IC	0	0	0	0

* See Fig. 4

** See Eq. (27) for definition of γ

For the plate portion the normal, shear and moment quantities per unit of circumferential length are

$$\bar{N}_p = \frac{D_p P_0 R_0}{\rho C^2} \left[\frac{\partial W_r}{\partial r} + \nu_p \frac{W_r}{r}\right] \tag{20}$$

$$\bar{Q}_p = \frac{D_p P_0 R_0}{\rho C^2} \alpha_p \left[\frac{\partial^3 W_z}{\partial r^3} + \frac{1}{r} \frac{\partial^2 W_z}{\partial r^2} - \frac{1}{r^2} \frac{\partial W_z}{\partial r}\right] \tag{21}$$

$$\bar{M}_p = \alpha_p \frac{D_p P_0 R_0^2}{\rho C^2} \left[\frac{\partial^2 W_z}{\partial r^2} + \frac{\nu_p}{r} \frac{\partial W_z}{\partial r}\right] \tag{22}$$

See Table 1, item 4 for definition of the corresponding non-dimensional and dimensional quantities.

1. Shell-Plate Connection

Equations (10)-(14) describe velocities at structure points providing no restriction is made concerning the relative angle between the shell wall and the plate bottom. If a right angle is to be maintained at this joining then the equation is modified for points near the corner.

The condition of a right angle at the shell-plate interface is stated by the constraint condition

$$G = \left[\frac{\partial W_r}{\partial z} + \frac{\partial W_z}{\partial r}\right]_{\substack{z=\ell \\ r=r_{LC}}} = 0 \tag{17}$$

the subscript "LC" defines the point at the interface, see Fig. 4. This is introduced into the variational procedure by the Lagrangian multiplier Λ such that the total variational expressions are

$$\frac{\partial(U_s + U_p)}{\partial W_{m_L}} + \Lambda \frac{\partial G}{\partial W_{m_L}} = 0 \tag{18}$$

where W_{m_L} indicates displacement at point "L" in either the r-direction, or the z-direction, and U_s, U_p are the total energy expressions given in Eqs. (8) and (9). For convenience the energy variation is written as

$$\frac{\partial(U_s + U_p)}{\partial W_{m_L}} = -A_{m_L} + \frac{\Delta V_{m_L}}{\Delta\tau} \tag{19}$$

[where the quantities A_m^L are given in Eqs. (11)-(14)] and the constraint, Eq. (17), is written in finite difference form

$$G = (W_{r_{LC}} - W_{r_{LC-1}}) \frac{\Delta r}{\Delta z} + W_{z_{LC}} - W_{z_{LC+1}} = 0 \qquad (20)$$

Then Eqs. (18), (19) and (20) combine to give

$$\frac{\Delta V_r^{LC-1}}{\Delta \tau} = \frac{\Delta r}{\Delta z} \Lambda + A_{r_s}^{LC-1} \qquad (21)$$

$$\frac{\Delta V_r^{LC}}{\Delta \tau} = - \frac{2}{1 + \gamma} \frac{\Delta r}{\Delta z} \Lambda + A_{r_s}^{LC} + A_{z_p}^{LC} \qquad (22)$$

$$\frac{\Delta V_z^{LC}}{\Delta \tau} = - \frac{2}{1 + \gamma} \Lambda + A_{z_s}^{LC} + A_{z_p}^{LC} \qquad (23)$$

$$\frac{\Delta V_z^{LC+1}}{\Delta \tau} = \frac{r_{LC}}{\gamma r_{LC+1}} \Lambda + A_{z_p}^{LC+1} \qquad (24)$$

A fifth equation, which allows for solution of Λ is obtained from the second derivative with respect to time of Eq. (19)

$$\frac{\partial^2 G}{\partial \tau^2} = \left(\frac{\Delta V_r^{LC}}{\Delta \tau} - \frac{V_r^{LC-1}}{\Delta \tau}\right) \frac{\Delta r}{\Delta z} + \frac{\Delta V_r^{LC}}{\Delta \tau} - \frac{\Delta V_z^{LC+1}}{\Delta \tau} = 0 \qquad (25)$$

Combining Eqs. (20)-(24) yield

$$\Lambda = \frac{\frac{\Delta r}{\Delta z}(A_{r_s}^{LC} + A_{r_p}^{LC} - A_{r_s}^{LC-1}) + A_{z_s}^{LC} + A_{z_p}^{LC} + A_{z_p}^{LC} - A_{z_p}^{LC+1}}{\frac{2}{1+\gamma}\left[1 + \left(\frac{\Delta r}{\Delta z}\right)^2\right] + \left(\frac{\Delta r}{\Delta z}\right)^2 + \frac{1}{\gamma}\frac{r_{LC}}{r_{LC+1}}} \qquad (26)$$

where

$$\gamma = \frac{D_p}{D_s} \frac{\Delta r}{\Delta z} \frac{\omega_s^2}{\omega_p^2} r_{LC} \qquad (27)$$

See Fig. 4 for points corresponding to superscripts LC, LC+1, LC-1, etc. In a layered medium it is understood that the Δz term appearing in equations related to the maintenance of a right angle at the corner

should be the value of the Δz in that layer in which the plate sits.

For a structure in which there is no right angle restriction at the corner the equations of motion for all points are given by Eq. (10). For a structure with a right angle restriction Eqs. (21)-(24) must be used as equations of motion for points LC-1, LC and LC+1. All other points are described as before.

III THE POSSI CODE

A. Conditions for use

Among the options built into the Possi Code is a choice of location and type of loading. There are three possibilities; loading on the upper boundary, see Fig. 5a; loading on the interior of the cavity (or structure, if it is present), Fig. 5b; loading on both the upper boundary and the cavity interior, Fig. 5c. In each case a time variation may be combined with an appropriate space variation, as shown. The input parameter controlling which of the three loading types is to be used is ILOAD. See card #2, Table 7. The actual loading function is to be input directly into program functions APSGZ and SIGAP as described in the next section. If no load is applied on either the upper or cavity boundary conditions of zero stress are assumed. It should be noted that boundary conditions at maximum grid lines are the type of transmitting boundary obtained from mirror image values of stress and velocity. Conditions along a line through the origin, but below the cavity are, of course, those of zero velocity in the radial direction.

The other options, such as non-dimensional versus dimensional computations, number of layers, lined or unlined cavity, right angle at shell-plate interface, graphic or printed output, are also controlled by input parameters which are listed in detail in Table 7, Appendix A.

The options of one dimensional (r-t or z-t) computations are activated by choice of grid dimensions. For a one dimensional r-t computation choose a long slender cavity with loading on the interior vertical surface as p(t), and a wide grid. For a one dimensional z-t computation

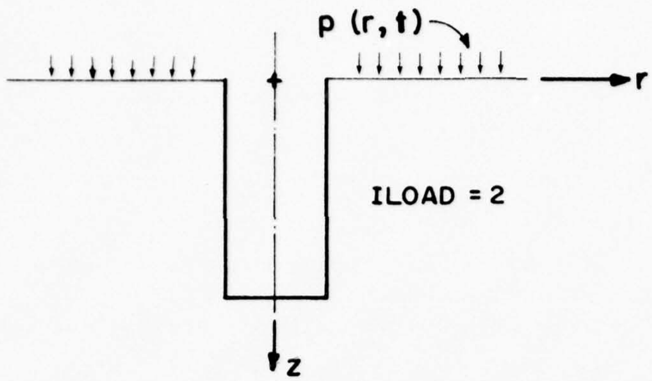

FIG.5a LOADING ON UPPER BOUNDARY

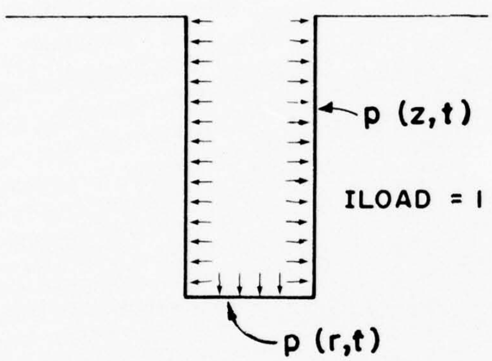

FIG. 5b LOADING ON INTERIOR OF CAVITY

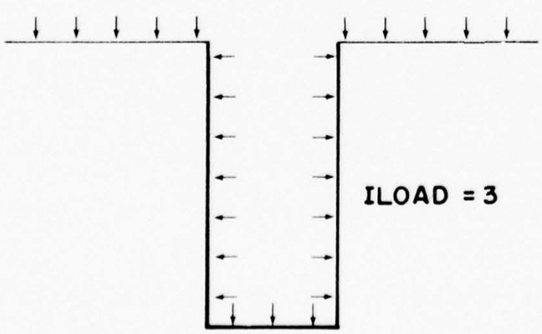

FIG. 5c COMBINED LOADING

LOADING OPTIONS FOR POSSI CODE

choose a p(t) loading on the upper boundary, a long slender cavity with no loading and a deep grid.

The numbering system used to identify points in the field and points on the shell is shown in Fig. 6. Special note should be made of the fact that field points are numbered (in the r-direction) from the first point away from the cavity, rather than from the origin, except at points below the cavity where numbering does begin from the origin. Regardless of grid dimensions chosen there should be at least 5 points on the vertical boundary of the cavity and at least 5 points on the horizontal boundary from $r=0$ to $r=r_{LC}$ at the bottom of the cavity.

Without precise stability criteria, it is recommended that time and space increments be chosen such that the quantity $\frac{\lambda_{max} \Delta t}{\Delta r}$ is well below 1.0 when there is no structure, and below when a shell-plate structure is present.

Typical compile time on a CDC 6600 is approximately 11 seconds. Typical run time for a 60 by 40 point grid, with three horizontal layers and no structure, running 300 time steps with printed output every 10th time step, and output for time history plots every 2nd time step is about 380 seconds. Typical run time for a 60 by 40 grid with one layer and a structural lining, running 200 time steps with the same frequency of output as above is about 220 seconds. Additional output will, of course, increase running times noticeably.

It may also be noted here that all input is on TAPE 2, all printed output is on TAPE 3, and all output for graphing is on TAPE 4.

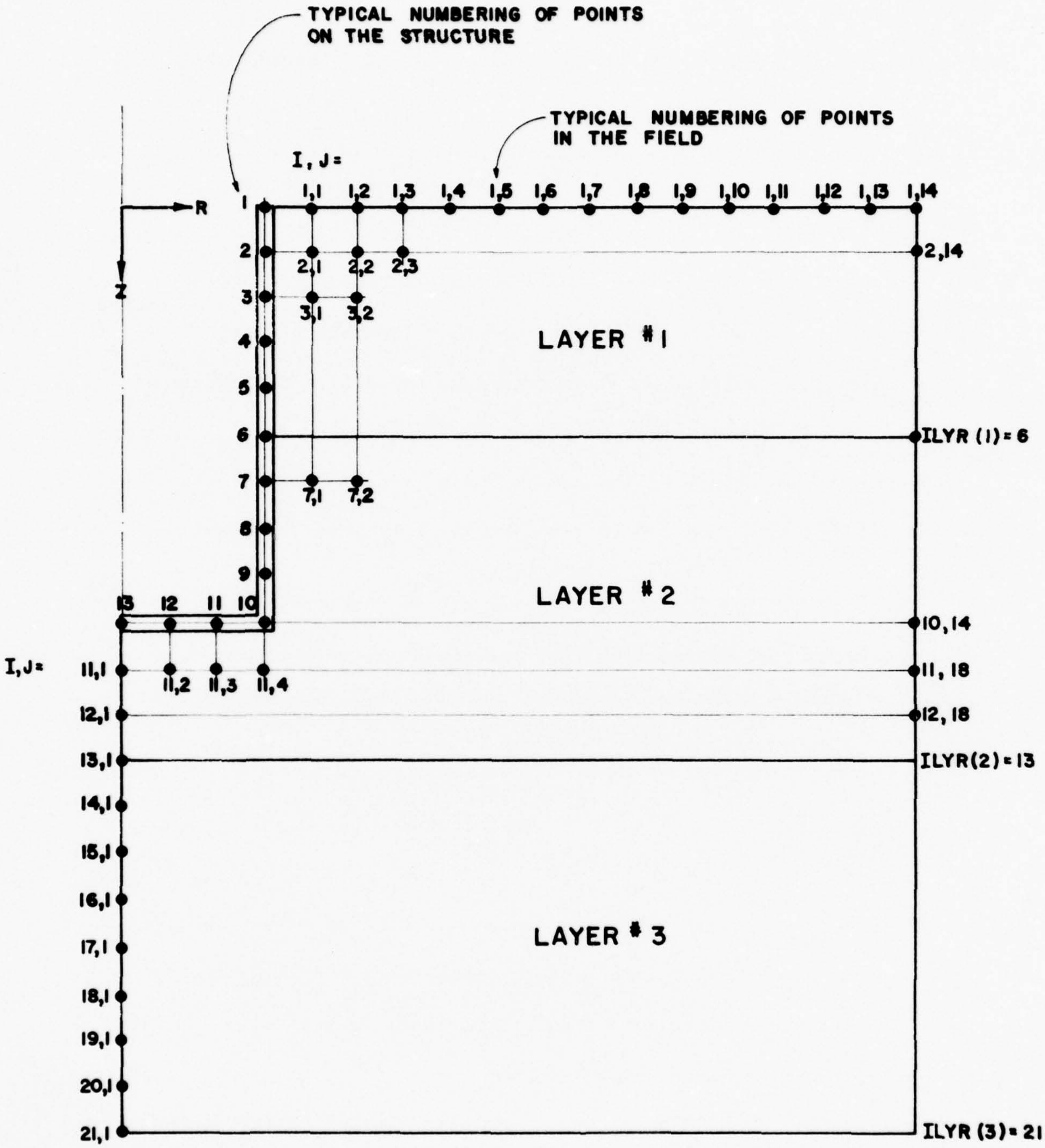

TYPICAL NUMBERING OF POINTS ON THE STRUCTURE
TYPICAL NUMBERING OF POINTS IN THE FIELD
I, J =
R
Z
1,1 1,2 1,3 1,4 1,5 1,6 1,7 1,8 1,9 1,10 1,11 1,12 1,13 1,14
1 2 3 4 5 6 7 8 9 10 11 12 13
2,1 2,2 2,3
3,1 3,2
2,14
LAYER # 1
ILYR (1) = 6
7,1 7,2
LAYER # 2
10,14
I, J =
11,1 11,2 11,3 11,4
11, 18
12,1
12, 18
13,1
ILYR(2) = 13
14,1 15,1 16,1 17,1 18,1 19,1 20,1 21,1
LAYER # 3
ILYR (3) = 21

FIG. 6

There are a few programming features which users of the POSSI code may wish to modify for certain types of computations. For instance, the way the code is presently written a velocity cutoff of $V = \left| \sqrt{V_z^2 + V_r^2} \right| = .001$ controls the extent of the computational field for a disturbance moving outwardly from the cavity. See comments in the next section, Description of Subroutines, Subroutine LOCATE. Also, currently the code allows for only three cycles of load, unload, reload. Three cycles were sufficient for the computations done thus far. See comments in the next section under Subroutine TEST, and see Fig. 8.

B. DESCRIPTION OF SUBROUTINES

The following describes the essential function of each subroutine in the POSSI Code. The Subroutines are listed in the order in which they are compiled in the code

RZ2D - MAIN

Increments time. Activates integration first in the r-direction (CALL RDIR), then in the z-direction (CALL ZDIR). If a structure is present with a right angle restriction at its corner, RZ2D - MAIN corrects the shell corner motion for that restriction. Integrates velocities into displacements, Eqs. (15), (16) at grid points on the structure. Calls for check of loading, unloading, reloading conditions at all field points (CALL TEST). Initiates graphic (CALL GRAPHS) or printed (CALL SLOT) output as required.

LOCATE

Computes arrays LR, LRMX which control the extent of integration in the r-direction, and arrays LZ, LZMX which control the extent of integration in the z-direction. At each time step the value of $V = \left| \sqrt{V_r^2 + V_z^2} \right|$ is computed at each field point with coordinates I, J. As long as a velocity $V > .001$ is encountered the arrays are set as $LR(I) = J + 1$, $LZ(J) = I + 1$. The values LRMX, LZMX are then set as $LRMX = \max LR(I)$, $LZMX = \max LZ(J)$. This criterion was selected for disturbance expanding outward from the cavity, and for essentially non-dimensional computations where $V \approx 1.0$. For other shape disturbances or for some dimensional computations where very large or very small V's are expected this criteria should be changed.

DATA

Requests input data according to specifications listed in Table 6. Initiates computation of constants (CALL CONST). Outputs all pertinent computational parameters as shown in the sample computations, Section IV.

CONST

Initializes arrays. All stresses and velocities are set to zero Computes constants CNR1...CNR12, arrays CLD, CS, CUN as defined in the list of common variables in Appendix C. Computes other constants from input data which are basic to the code.

RDIR

Integrates equations of motion in the r-direction, at all field points, by evaluating the upper set of equations shown in Table 2. First integration is done in Region 1 as shown in Fig. 7a. Then Subroutine SHELL is called at the end of each I^{th} line of integration to perform the integration of the shell equations of motion in both the r- and z-directions, (if there is a structure), or to compute the motion of field points at an applied pressure boundary, if there is no structure. If a structure is present, all its mass is considered to be distributed along the line defining the cavity, and all motions of points on that line are goverened by the structural equations of motion. If no structure is present the line defining the cavity is all material and requires integration of the field equations in both the r- and z-directions. Therefore, in the case of no structure, r-direction integration in Region 1, Fig. 7a is followed by r-direction integration along the bottom boundary of the hole, (CALL PLATR), which is then followed by r-direction integration in Region 2, Fig. 7a.

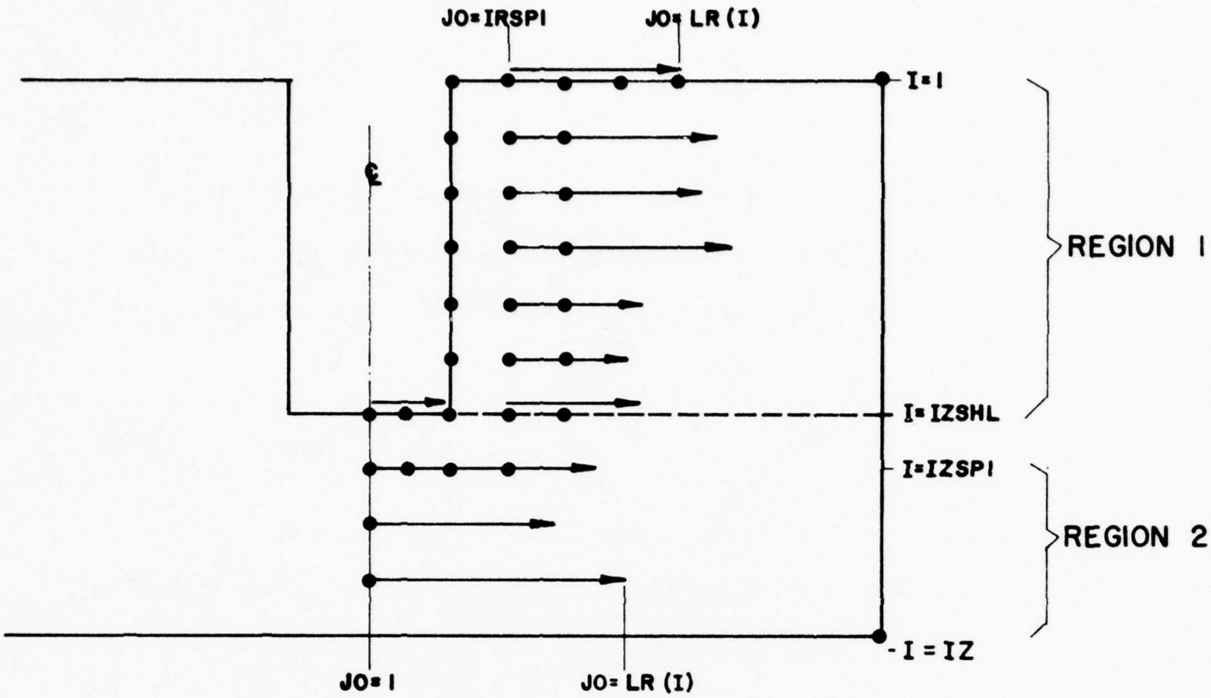

JO=IRSPI
JO=LR(I)
I=1
REGION 1
I=IZSHL
I=IZSPI
REGION 2
I=IZ
JO=1
JO=LR(I)

FIG. 7 a

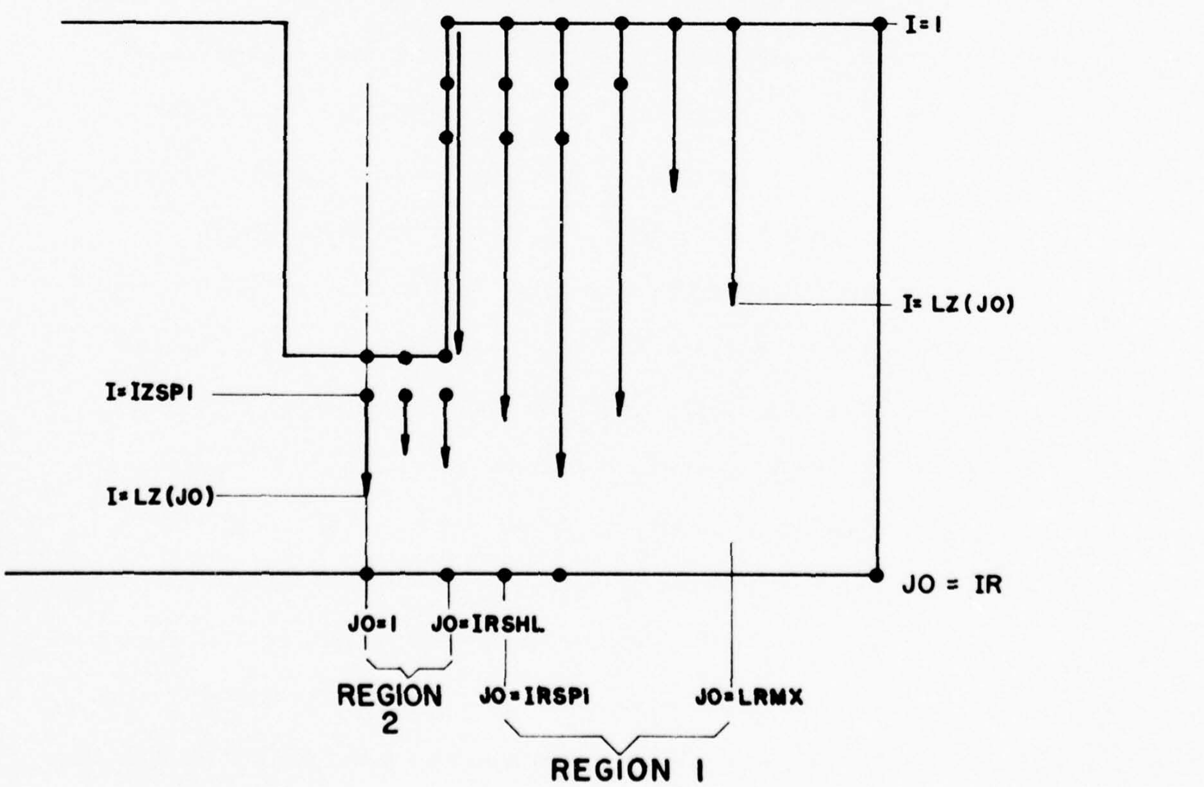

I=1
I=LZ(JO)
I=IZSPI
I=LZ(JO)
JO=IR
JO=1
JO=IRSHL
REGION 2
JO=IRSPI
JO=LRMX
REGION 1

FIG. 7 b

ZDIR

Integrates equations of motion in the z-direction at all field points by evaluating the lower set of equations shown in Table 2. First the integration is done in Region 1, Fig. 7b, then the integration is done in Region 2. At the end of each $J0^{th}$ line of integration in Region 2 Subroutine PLATE is called to provide the integration of the plate equations of motion in both the r- and z-directions (if there is a structure), or to compute the field integration at points on an applied pressure boundary, if there is no structure. Then, if no structure is present, for the reasons stated above, integration of the field equations along the vertical cavity boundary is initiated by calling subroutine SHELZ.

UPBND

Integrates the equations of motion in the z-direction at field points along the upper, $z = 0$, boundary. Calls function APSGZ for applied stress boundary condition.

SHELL

Evaluates the equations of motion for the shell, as given in Tables 3a and 3b, if a structure is present. If the cavity is unlined, the field equations of motion are integrated in the r-direction for an applied stress boundary condition. The function SIGAP is called for application of σ_r to the inner surface of the cavity or shell, ($\sigma_{rz} = 0$ is always assumed on this surface).

SHELZ

Integrates the field equations of motion in the z-direction along the vertical boundary of the cavity. This subroutine is activated only if the cavity is unlined.

PLATE

Evaluates the equations of motion for the plate as given in Tables 4a and 4b, if a structure is present. If the structure is unlined, the field equations of motion are evaluated in the z-direction for an applied stress boundary condition. The function SIGAP is called for an applied stress in the z-direction on the inner surface of the plate or the unlined cavity. (Again $\sigma_{rz} = 0$ is assumed on this surface.)

PLATR

Integrates the field equations of motion in the r-direction along the horizontal boundary of the cavity. This subroutine is activated only if the cavity is unlined.

COEFFS

Sets the coefficient arrays C and CS to the appropriate values for each layer. Sets the coefficient array C at each field point to loading or unloading values as determined by the value of the indicator KODES.

TEST

At each point in the field the new value of the first invariant AJ1 is tested against the last previous compressive maximum AJ1MX. Depending upon the outcome of this test the indicator KODES is given a numerical value to indicate conditions of loading, unloading/reloading as listed in Table 7, and shown graphically in Fig. 8. Providing for three cycles of load/unload was sufficient for the computations done so far. The user may find, for certain loadings, further cycling should be provided for.

NUVALS

The evaluation of equations given in Table 2 involves updating of quantities at each field point. L, from non updated quantities at L-1 and L+1. As the integration proceeds forward in either the r- or z-direction

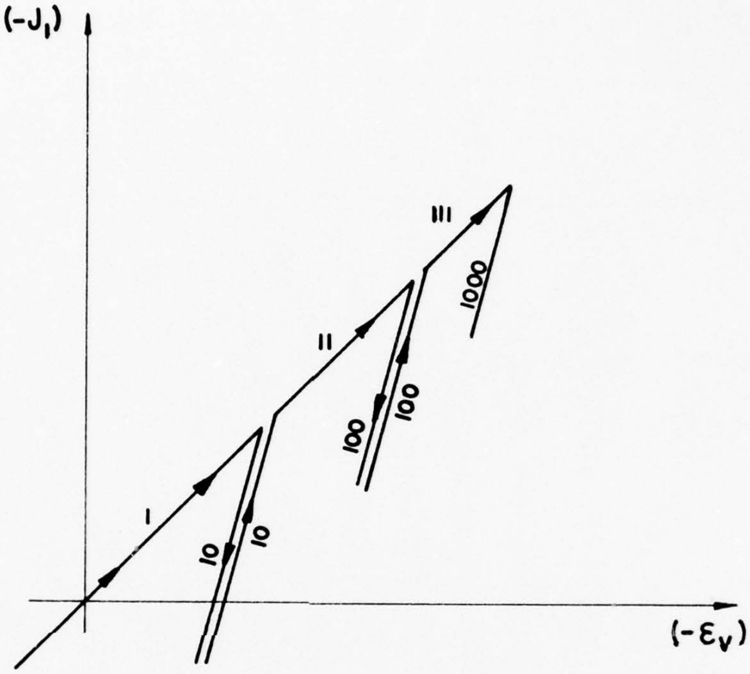

FIG. 8 VALUES OF KODES

the updated quantities at "L" are stored in a set of temporary arrays (TSR, TSZ, TSRZ, TVR, TVZ, TAJ1) until the updated quantities at L+1 are evaluated and stored temporarily. Then this subroutine NUVALS places the temporary arrays from point L into the final arrays (SGR, SGZ, SGRZ, VR, VZ, AJ1) of stress and velocity at point "L". This flip-flopping minimizes the amount of memory required in the integration.

SHLNU

Performs the same function that NUVALS does, only for quantities being integrated along the cavity boundary in SHELZ and PLATR.

SIGAP

Function which sets the value of applied normal stress on the interior boundary of the cavity or the structure, as a function of time and location. Applied pressure is to be considered positive in this function. Each time a different applied pressure function is to be considered, the statements in this function must be changed.

APSGZ

Function which sets the value of applied normal stress on the upper boundary , Z=0. See comments under SIGAP.

SLOT

Directs printed output, of computations, samples of which are shown in Appendix B. All output from SLOT is on TAPE 3.

GRAPHS

Accumulates output for later use by plotting subroutines. All output from GRAPHS is on TAPE 4.

Table 5 - Indicators for Loading, Unloading and Reloading

KODES	CONDITION	COMPUTATIONAL PARAMETERS
1	Initial virgin loading	$C_{p_{LD}}$, C_s, ν_{LD}
10	Unload from first compressive J_1 maximum, or reload up to that value $(-J_1) \leq (-J_1)^{(1)}_{max}$	$C_{p_{UN}}$, C_s, ν_{UN}
11	Second virgin loading $(-J_1) > (-J_1)^{(1)}_{max}$	$C_{p_{LD}}$, C_s, ν_{LD}
100	Unload from second compressive J_1, or reload up to that value $(-J_1) \leq (-J_1)^{(2)}_{max}$	$C_{p_{UN}}$, C_s, ν_{UN}
111	Third virgin loading	$C_{p_{LD}}$, C_s, ν_{LD}
1000	Unload from third compressive J_1 or reload	$C_{p_{UN}}$, C_s, ν_{UN}

IV REPRESENTATIVE RESULTS

A. Case with layered medium, no structure.

Computations were done for the three-layered medium with no structure, shown in Fig. 9. The material parameters for this case are the same as those used for computations in a three layered medium with an unlined cavity discussed in Ref. [3]. The loading on the interior of the cavity is a triangular pulse in time, Fig. 10a, but in this case has an exponential variation of $e^{-.2z}$ (Fig. 10b) as opposed to the space independent pulse that was used in Ref. [3]. Quantities were computed in non-dimensional form, and graphic output was obtained for radial velocity near the mid-point of each layer at $r = 2.0$.

A sample of portion of POSSI code output is shown in Fig. 11. Listed in this figure are all the input quantities required for the computation of Case A results.

Radial velocity time histories at points near the mid-point of each layer, at $r = 2.0$ are shown in Fig. 12. The relative differences in arrival times are of course due to the different loading speeds in the three layers (1.0/1.091/5.145). The decreasing magnitude of velocity, with depth represents the response to the spatial distribution of the loading function. The relative length of time of a full pulse in each layer is due to the difference in unloading wave speeds in the three layers (2.4/3.325/6.417).

A stress profile of σ_r versus z-direction is shown in Fig. 13. Here the existence of layers is evident, the discontinuity of radial stress at each interface shows only approximately because the interface line has been chosen, arbitrarily, to sit in the upper rather than the lower

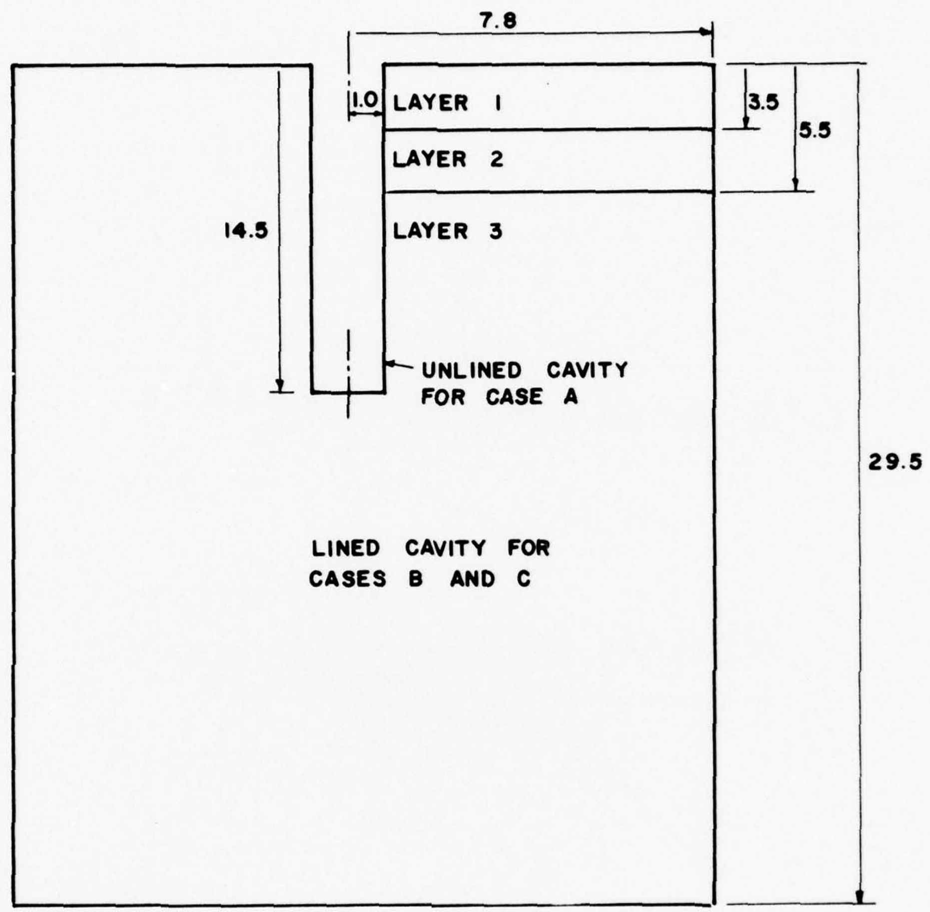

FIG. 9 CONFIGURATION FOR COMPUTATIONS

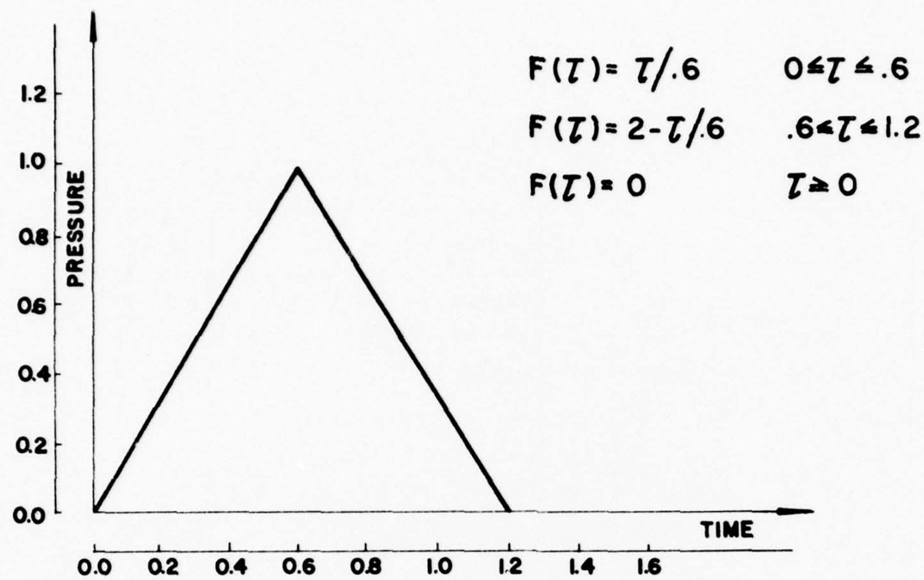

FIG. 10a F(τ)

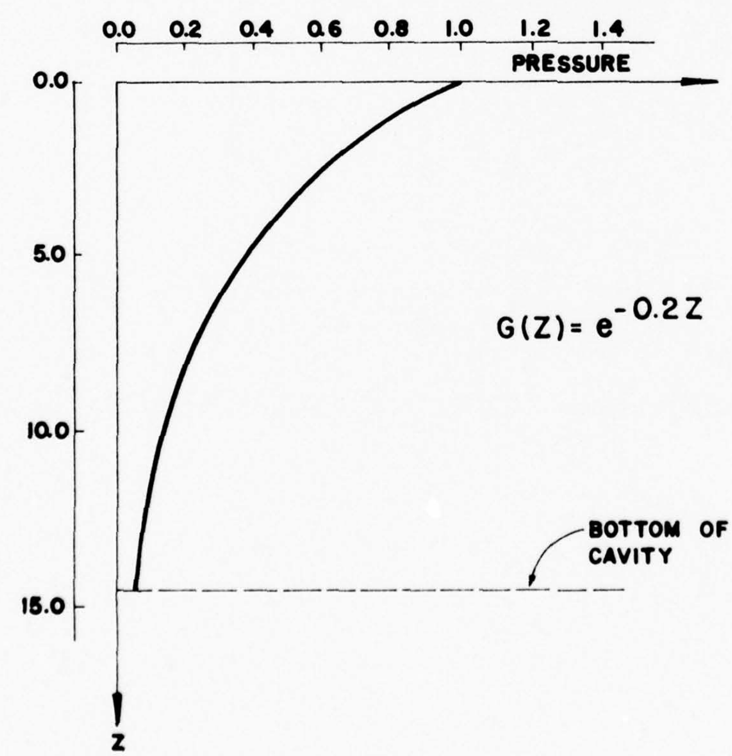

FIG. 10bG(z)

```
BILINEAR SOLID, TWO-DIMENSIONAL OUT-GOING WAVE IN CYLINDRICAL COORDINATES WITH R-Z VARIATION ONLY
NO SHELL, 3 LAYER, TRIANGLE LOAD WITH EXP(-.2*Z) DEPTH VARIATION

PARAMETERS FOR COMPUTATION

                    DR =    .20000            DT =    .01500

                    MAX RADIUS OF GRID =    7.800          MAX DEPTH OF GRID =  29.500

                    OUTPUT EVERY   10TH TIME STEP, UP TO A MAXIMUM OF  200 STEPS
                    NUMBER OF POINTS ON PLATE IN R-DIRECTION =    6
                    NUMBER OF POINTS ON SHELL IN Z-DIRECTION =   30

                    NUMBER OF POINTS IN FIELD IN R-DIRECTION =   40
                    NUMBER OF POINTS IN FIELD IN Z-DIRECTION =   60

                    OUTPUT POINTS ON SHELL AT I =    4,  10,  21,  28,  29,  30,  31
                                                    32,  35,

                    OUTPUT POINTS IN THE FIELD AT (I,J) =   (  4,  5)( 10,  5)( 21,  5)
                                                            (  4, 10)( 10, 10)( 21, 10)

RESULTS COMPUTED IN NON-DIMENSIONAL FORM

LOADING ON INTERIOR OF CAVITY

HOLLOW CAVITY, NO SHELL
                    CAVITY RADIUS =    1.00
                    CAVITY LENGTH =   14.500

MATERIAL PROPERTIES, FOR  3 LAYERS
```

LAYER	NLYR	DZ	LAMBDA LOAD	LAMBDA UNLOAD	LAMBDA SHEAR	NU LOAD	NU UNLOAD	Z MAX	DENSITY RATIO
1	8	.500	1.000	2.400	.594	.223	.467	3.500	1.000
2	12	.500	1.091	3.325	.594	.286	.484	5.500	1.000
3	60	.500	5.145	6.147	2.970	.250	.364	29.500	1.000

```
TIME HISTORIES TO BE PLOTTED EVERY  2TH TIME STEP
                                        VARIABLE    LOCATION
                                         NUMBER      I    J
                    POINTS ON THE SHELL
                                           4         4
                                           4        10
                                           4        21
                    POINTS IN THE FIELD
                                           4         4    5
                                           4        10    5
                                           4        21    5

SPACE PROFILES TO BE PLOTTED            VARIABLE    TIME      LINE
                                         NUMBER     STEP    LOCATION
                    IN THE R-DIRECTION
                    IN THE Z-DIRECTION
                                           1        150        11
```

J	R	Z	KODE	SIGMA R	SIGMA Z	SIGMA RZ	R VEL	Z VEL	R DISPL	Z DISPL	J 1	J 1 MAX	APPLD LOAD

```
    IT =  10     T =    .150
```

FIG. 11

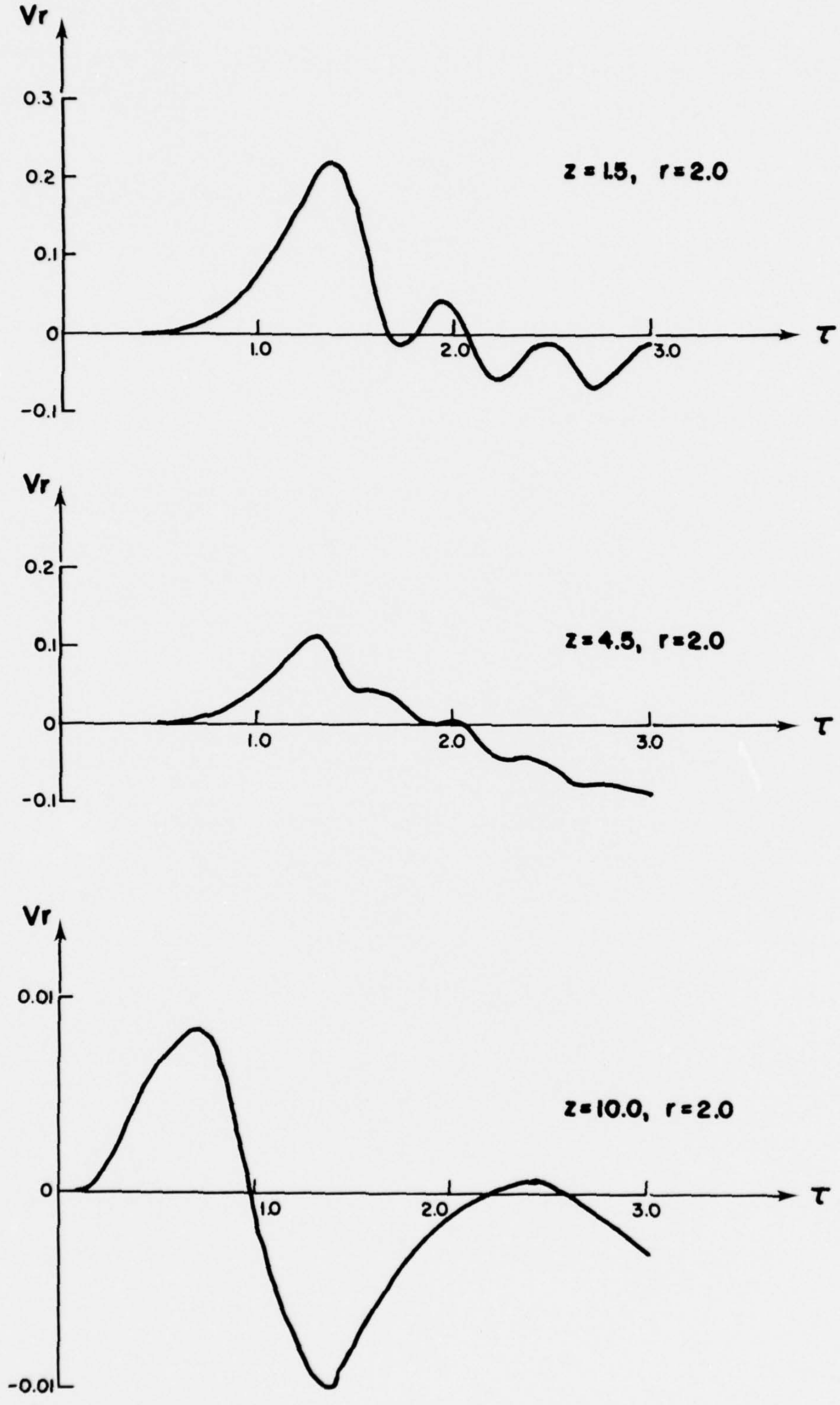

FIG. 12 VELOCITY TIME HISTORIES
CASE A – NO SHELL

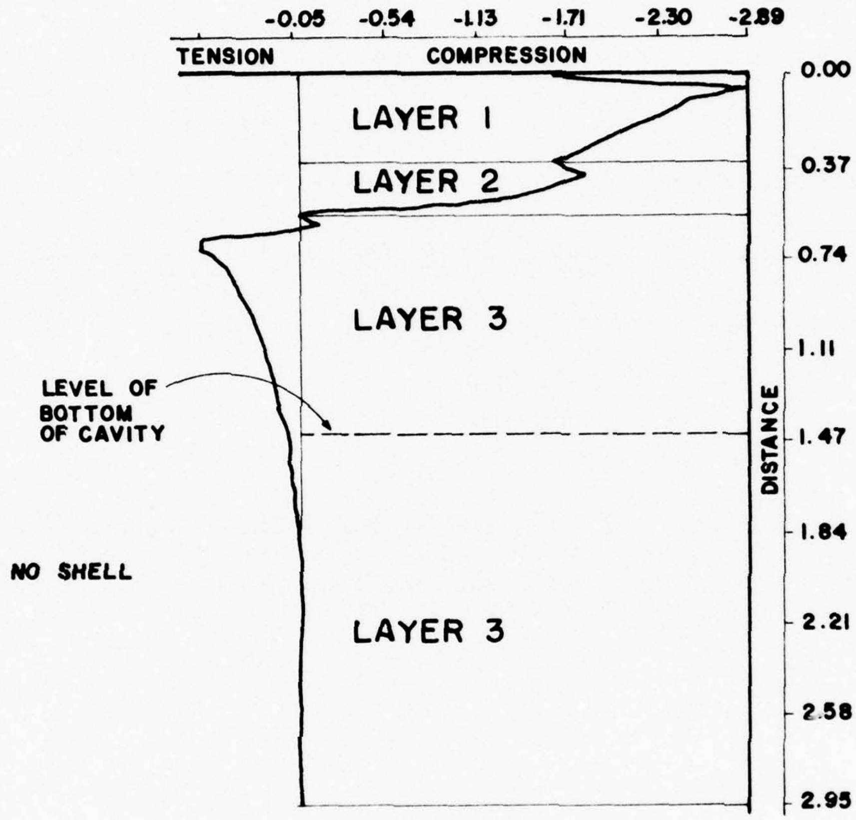

FIG.13 STRESS PROFILE IN THE Z-DIRECTION AT R= 3.0 , T= 1.5

CASE A, NO SHELL

layer. The computation scheme permits only one medium to exist along any grid line.

B. Case with structure (non-dimensional)

For a second set of representative computations a structure was added to the material configuration of Case A. The same loading, Figs. 10a, 10b, was applied, this time to the interior of the strucuture. Output was obtained at the same space points as in Case A.

Figure 14 gives the initial POSSI code print out which lists all the parameters, both material and structural for this case. The structural parameters are the same as those used for the structure discussed in Ref. [4].

Figure 15 presents radial velocity-time histories at the same points as for Case A. The effect of the mass of structure, one radii removed from it, is apparent from the reversal of the initially outwardly directed V_r.

C. Case with structure (dimensional)

The input parameter chosen for this case were similar to those used for the runs in Ref. [4]. They are

$$p_0 = 10.2 \ \#/\text{in}^2$$

$$R_0 = 52000 \text{ inches}$$

$$C = 52000 \text{ inches/sec}$$

$$\rho = .0001947 \ \frac{\#\text{sec}^2}{\text{in}^4} \ (130 \ \#/\text{ft}^3)$$

$$h_s = h_p = 3380 \text{ inches}$$

$$\Omega_s = \Omega_p = 4.0 \text{ rps}$$

$$\frac{\Delta R}{R_0} = 0.2$$

```
BILINEAR SOLID, TWO-DIMENSIONAL OUT-GOING WAVE IN CYLINDRICAL COORDINATES WITH R-Z VARIATION ONLY
3 LAYERS WITH SHELL-PLATE LINING, RIGHT ANGLE,TRIANGLE WITH E-.22 LOAD

 PARAMETERS FOR COMPUTATION

                    DR =   .20000           DT =   .01000

                    MAX RADIUS OF GRID =   7.800           MAX DEPTH OF GRID =  29.500

                    OUTPUT EVERY   10TH TIME STEP, UP TO A MAXIMUM OF   300 STEPS
                    NUMBER OF POINTS ON PLATE IN R-DIRECTION =     6
                    NUMBER OF POINTS ON SHELL IN Z-DIRECTION =    30

                    NUMBER OF POINTS IN FIELD IN R-DIRECTION =    40
                    NUMBER OF POINTS IN FIELD IN Z-DIRECTION =    60


                    OUTPUT POINTS ON SHELL AT I =   4,  10,  21,  28,  29,  30,  31
                                                   32,  35,   1,   2,   3,

                    OUTPUT POINTS IN THE FIELD AT (I,J) =  (  4,  5)( 10,  5)( 21,  5)


 RESULTS COMPUTED IN NON-DIMENSIONAL FORM

 LOADING ON INTERIOR OF CAVITY

 CAVITY BOUNDARY WITH SHELL
                    RIGHT ANGLE MAINTAINED AT PLATE-SHELL CONNECTION

 PROPERTIES OF THE STRUCTURE

                         THICKNESS    NU        E        OMEGA    DENSITY

                    SHELL      .0650    .2500   .30E+08    4.0000    3.6700
                    PLATE      .0650    .2500   .30E+08    4.0000    3.6700

                    CAVITY RADIUS =   1.00
                    CAVITY LENGTH =  14.500

 MATERIAL PROPERTIES, FOR  3 LAYERS

 LAYER   NLYR       DZ      LAMBDA    LAMBDA    LAMBDA       NU         NU      Z MAX      DENSITY
                             LOAD     UNLOAD     SHEAR      LOAD      UNLOAD               RATIO

   1       8       .500     1.000     2.400      .594      .223       .467     3.500      1.000
   2      12       .500     1.091     3.325      .594      .286       .484     5.500      1.000
   3      60       .500     5.145     6.417     2.970      .250       .364    29.500      1.000


 OUTPUT FOR TIME HISTORY PLOTS EVERY  2TH TIME STEP
                                       VARIABLE    LOCATION
                                        NUMBER      I    J
                    POINTS ON THE SHELL
                                          5         7
                                          6        10
                                          6        21
                                          6        30
                                          7        30
                                          7         4
                    POINTS IN THE FIELD
                                          4         4    5
                                          4        10    5
                                          4        21    5

 SPACE PROFILES TO BE PLOTTED          VARIABLE     TIME      LINE
                                        NUMBER      STEP    LOCATION
                    IN THE R-DIRECTION
                                          4         150        4
                                          4         150       10
                                          4         150       21
                                          2         150       11
                    IN THE Z-DIRECTION


 I   J     R       Z   KODE  SIGMA    SIGMA    SIGMA      R       Z       R       Z       J 1     J 1    APPLD   SIGMA
                               R        Z       RZ       VEL     VEL    DISPL   DISPL           MAX     LOAD    THETA

        IT =  10     T =    .100
```

FIG. 14

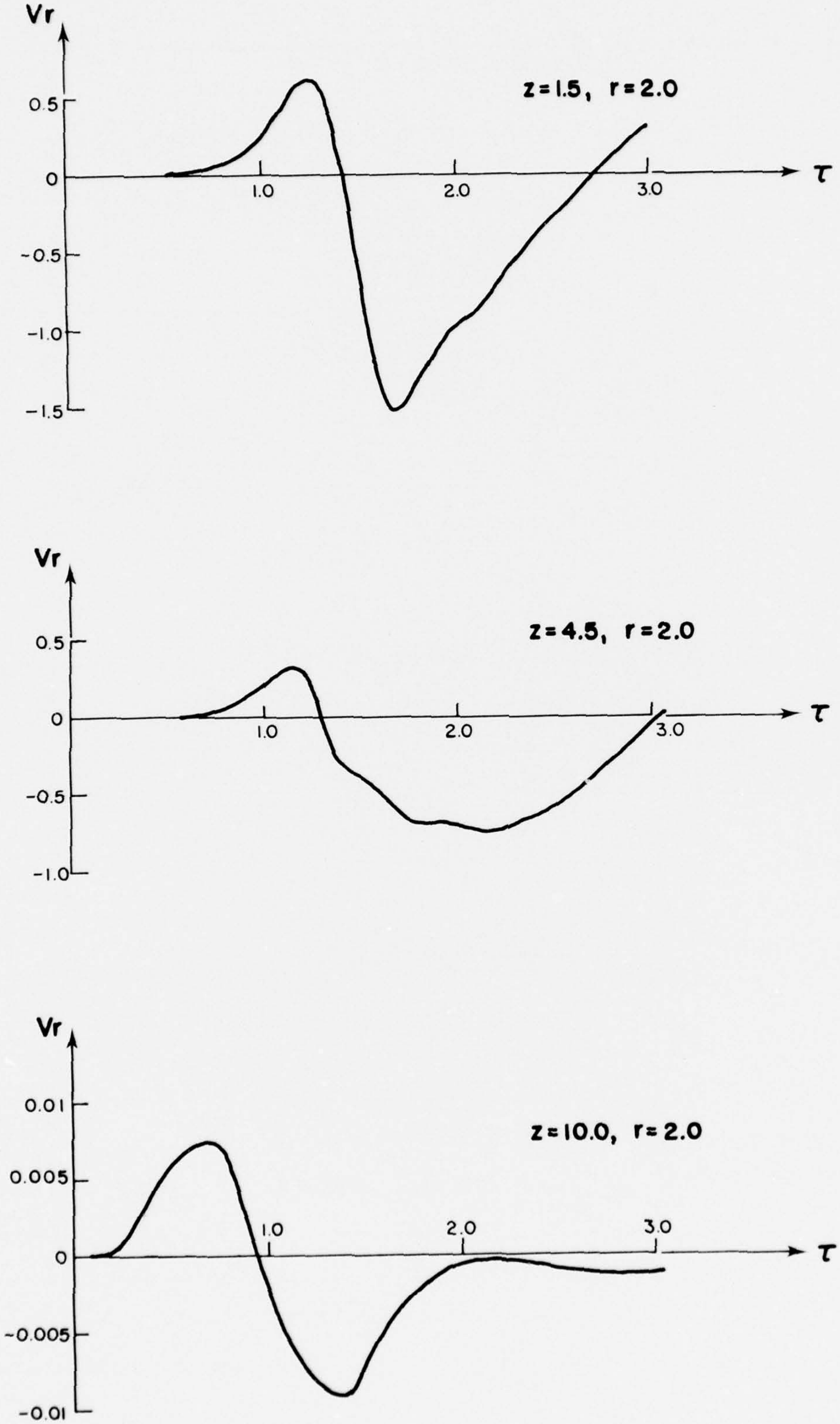

FIG. 15 VELOCITY TIME HISTORIES
CASE B - WITH SHELL

$$\Delta t = 0.01 \text{ sec}$$

$$\frac{\Delta Z}{R_0} = 0.5$$

Since the non-dimensionalizing factor $\frac{\rho C}{P_0} = 1.0$ the velocities shown in Fig. 15 may be interpreted as velocity output for this case. The units on the velocity scale in this case would be in inches/sec, and the time scale would be in seconds. A sample of the computer output of input information is shown in Fig. 16.

BEST AVAILABLE COPY

```
BILINEAR SOLID, TWO-DIMENSIONAL OUT-GOING WAVE IN CYLINDRICAL COORDINATES WITH R-Z VARIATION ONLY
3 LAYERS WITH SHELL-PLATE LINING, RIGHT ANGLE,TRIANGLE WITH F-.22 LOAD

PARAMETERS FOR COMPUTATION

        DR =   .20000          DT =   .01000

        MAX RADIUS OF GRID =   7.000          MAX DEPTH OF GRID =  29.500

        OUTPUT EVERY   10TH TIME STEP, UP TO A MAXIMUM OF  300 STEPS
        NUMBER OF POINTS ON PLATE IN R-DIRECTION =    6
        NUMBER OF POINTS ON SHELL IN Z-DIRECTION =   30

        NUMBER OF POINTS IN FIELD IN R-DIRECTION =   40
        NUMBER OF POINTS IN FIELD IN Z-DIRECTION =   60

        OUTPUT POINTS ON SHELL AT I =   4,  10,  21,  28,  29,  30,  31
                                       32,  35,   1,   2,   3,

        OUTPUT POINTS IN THE FIELD AT (I,J) =  ( 4,  5)( 10,  5)( 21,  5)

RESULTS COMPUTED IN DIMENSIONAL FORM
        SPEED   = .5200E+05
        DENSITY = .1947E-03

        R ZERO  = .5200E+05

LOADING ON INTERIOR OF CAVITY

CAVITY BOUNDARY WITH SHELL
        RIGHT ANGLE MAINTAINED AT PLATE-SHELL CONNECTION

PROPERTIES OF THE STRUCTURE
```

	THICKNESS OVER R ZERO	NU	E	OMEGA	DENSITY RATIO
SHELL	.0650	.2500	.30E+08	4.0000	3.5285
PLATE	.0650	.2500	.30E+08	4.0000	3.5285

```
        CAVITY RADIUS =   1.00
        CAVITY LENGTH =  14.500

MATERIAL PROPERTIES, FOR  3 LAYERS
```

LAYER	NLYR	DZ	LAMBDA LOAD	LAMBDA UNLOAD	LAMBDA SHEAR	NU LOAD	NU UNLOAD	Z MAX	DENSITY RATIO
1	8	.500	1.000	2.400	.504	.223	.467	3.500	1.000
2	12	.500	1.091	3.325	.594	.286	.484	5.500	1.000
3	60	.500	5.145	6.417	2.970	.250	.364	29.500	1.000

```
OUTPUT FOR TIME HISTORY PLOTS TO BE EVERY  2TH TIME STEP
                                   VARIABLE   LOCATION
                                    NUMBER     I    J
        POINTS ON THE SHELL
                                      6        7
                                      6       10
                                      6       21
                                      6       30
                                      7       30
                                      7        4
        POINTS IN THE FIELD
                                      4        4    5
                                      4       10    5
                                      4       21    5

SPACE PROFILES TO BE PLOTTED        VARIABLE   TIME    LINE
                                     NUMBER    STEP   LOCATION
        IN THE R-DIRECTION
                                      4        150       4
                                      4        150      10
                                      4        150      21
                                      2        150      11

 I   J   R     Z     MODE  SIGMA R    SIGMA Z  SIGMA THETA  SIGMA RZ    J 1     J 1 MAX  APPLIED LOAD
                           R VELOCITY Z VELOCITY  R DISPL   Z DISPL
                                      SHELL N               SHELL M             SHELL Q
```

FIG. 16

V CONCLUSION

A description of a computer code known as POSSI has been presented. The code was written to provide a small, flexible tool for computing effects of a soil-structure interaction problem in two-dimensional (r, z) coordinates, where the cylindrical structure is buried in a type of dissipative material which may be layered. The POSSI code may be used as a check code for large finite element or finite difference computations, or it may be used to explore various soil-structure interaction problems (within the limitation of the type of material presented). It may also be used to efficiently run CIST type problems for cases in which the primary dissipation mechanism in the soil comes from pressure-volume hysteresis.

Results from two sample problems have been presented. The first being a long cylindrical hole, unlined, in a material of three layers. The second problem consisted of a structurally lined long cylindrical cavity in the same three layered material. In both cases results were present in non-dimensional form, input and output information from the code was provided for both. As a subcase to the second the results were also given in dimensional form.

In any computations using POSSI code there is certain care to be taken. Boundary and corner points present problems of approximation to real situations. Conclusions drawn about results at such points must be more carefully checked. Section III of this report lists some other points of care which should be taken when using the POSSI code.

Results from the two-dimensional r, θ coordinate problem for this configuration have already been presented, Ref. [2]. A recommended step in this work is to combine the computer code that was written for

the results of Ref. [2] with the POSSI code to produce a three-dimensional code for r, θ, z coordinates. Such a code would still be relatively small and flexible enough to be considered a check code. It would also provide a code for one of the few three-dimensional structure-medium interaction problems not restricted to being in an elastic material.

REFERENCES

[1] A.T. Matthews and H.H. Bleich, "Comparison of the Results of the Dynamic Response of Cylindrical Shells by Characteristic and by Finite Element Methods - Axisymmetric Case", Weidlinger Associates for Defense Nuclear Agency, February 1974.

[2] A.T. Matthews and H.H. Bleich, "Dynamic Response of Cylindrical Shells in Bilinear Media - Two-Dimensional Case", Weidlinger Associates for Defense Nuclear Agency, October 1974, DNA 3607Z.

[3] A.T. Matthews and H. H. Bleich, "Dynamic Response of a Cylindrical Cavity of Finite Length in a Bilinear Material", Weidlinger Associates for Defense Nuclear Agency, June 1975, DNA 3756T.

[4] A.T. Matthews and H.H. Bleich, "Dynamic Response of an Axisymmetric Lined Cylindrical Cavity of Finite Length in a Bilinear Material", Weidlinger Associates for Defense Nuclear Agency, April 1976, DNA 3997F.

APPENDIX A - INPUT INSTRUCTIONS FOR POSSI CODE

All input data required for the POSSI code is listed in Table 6 in the order in which it is required. Variable names, description and format for each card set are given. (Variable names are also defined in Appendix B.) Variables required for choice of options such as loading type, non-dimensional versus dimensional output, etc. are also listed.

Table 7 lists the numbering convention for each variable on the shell or in the field. If printed output or graphic output is desired the quantity to be output (stress, velocity or displacement) will be identified by this number system.

TABLE 6 - DESCRIPTION OF INPUT DATA FOR POSSI CODE (In the order in which it is required)

CARD SET	VARIABLE	DESCRIPTION	FORMAT
1	TITLE	Any alpha numeric description of the run being made. Total number of characters is 80.	8A10 one card
2	NLAYR ILOAD IR IZ NTIME	Number of layers = 1 for loading on cavity interior = 2 for loading on upper boundary = 3 for loading on both cavity interior and upper boundary Maximum number of mesh points in the R-direction. See Fig.7b Maximum number of mesh points in the Z-direction. See Fig.7a Maximum number of time steps to be run.	16I5 one card
3	NOSHL IRSHL IZSHL	= 0 if no structure lines the cavity = 1 if shell-plate structure lines the cavity Maximum number of mesh points on the plate (in the R-direction). See Fig.7b Maximum number of mesh points on the shell (in the Z-direction). See Fig.7a	16I5 one card
4	NPRT NPRSH NPAIR NORIT NODIM NGRPH	Output is printed every "NPRT" time step Total number of points around the cavity at which printed output is desired Total number of points in the field at which printed output is desired = 1 a right angle is preserved at the shell-plate connection = 0 no right angle is maintained = 0 all output is presented in non-dimensional form = 1 all output is in dimensional form = 0 no graphed output is desired = 1 yes, some graphs are to be printed	16I5 one card

CARD SET	VARIABLE	DESCRIPTION	FORMAT
	IF NODIM = 0 the following card is to be omitted		
5	DENSM SPEED RADIUS	Density of the material in the field Initial loading speed of P-waves in the material Nominal radius of the cavity These are reference values for internal non-dimensionalization. These three quantities should have consistent units. That is, all inches or all feet. Whichever is used will determine whether output occurs in [inches, inches/sec, psi] or [feet, ft/sec, psf] units	8F10 one card
6	ISHPR(NPR), NPR=1,NPRSH	Indices of mesh points on the cavity boundary where printed output is desired. See Fig. 6 for numbering order	16I5 one card for NPRSH $\leq$ 16
7	IPR(NPR), JPR,(NPR), NPR=1,NPAIR	I,J indices (in the Z and R-directions, respectively) of points in the field where printed output is desired. See Fig. 6 for the numbering order.	16I5 one card for (2*NPAIR) $\leq$ 16
	If NGRPH = 0 cards 9 through 11 are to be omitted. (That is, no graphed output is desired.)		
8	ITGRF MXGRS MXGRF MXPRF	Time history plots are made at every "ITGRF" time step The total number of time histories of points on the structure for which graphs are desired. The total number of time histories of points in the field for which graphs are desired. The total number of stress or velocity profiles in either the R- or Z-direction for which plots are desired.	16I5 one card
	If MXGRS = 0 the following card is to be omitted. (That is, no time histories of points on the structure are requested.)		

CARD SET	VARIABLE	DESCRIPTION	FORMAT
9	NSHV	The number of the structure variable for which a time history is desired. See Table 7 for the number used to represent each variable.	16I5 one card for each variable/point combination
	NSHPT	The number of the mesh point on the structure at which a time history is to be plotted. See Fig. 6	Total number of cards = MXGRS
	If MXGRF = 0 the following card is to be omitted. (That is, no time histories for points in the field are requested.)		
10	NFLV	The number of the field point variable for which a time history is desired. See Table 7 for the number used to represent each variable.	16I5 one card for variable/point combination
	IFLPT	The I,J mesh point numbers of the point in the field for which a time history is desired. See Fig. 6 for the numbering sequence used for field points.	Total number of cards = MXGRF
	If MXRPF = 0 the following card set is to be omitted. (That is, no space profiles are requested.)		
11	NVAR	The number of the field variable for which a space profile is desired.	16I5 one card for each set of four variable
	MTPT	The time step number at which the space profile is to be observed.	Total number cards = MXPRF
	NRORZ	= 1 If the space profile is to be taken in the R-direction = 2 If the space profile is to be taken in the Z-direction	
	LINE	The index number of the line along which the space profile is to be taken. If NRORZ = 1 (profile in the R-direction) then LINE will be a value fo the I index in the field. If NRORZ = 2 (profile in the Z-direction) then LINE will be a value of the J index in the field.	

CARD SET	VARIABLE	DESCRIPTION	FORMAT
14	LAMUN	Non-dimensional unloading wave speed λ_{UN}. See Table I	
	LAMS	Non-dimensional shear wave speed λ_s . See Table I	
	NULD	Poisson ratio for loading conditions	
	NUUN	Poisson ratio for unloading conditions	
	DENS	Material density, relative to DENSM.	

CARD SET	VARIABLE	DESCRIPTION	FORMAT
12	DT	Time increment in consistent time units with SPEED for a dimensional run.	8F10
	If NOSHL = 0 the following card set is omitted. (That is, if no structure lines the cavity.)		
13	HSH	Thickness of the shell	8F10
	HPL	Thickness of the plate	Last two quantities are put on a second card
	SHNU	Poisson ratio of material in the shell	
	PLNU	Poisson ratio of material in the plate	
	ESH	Young's modulus of material in the shell	
	EPL	Young's modulus of material in the plate	
	OMSH	Fundamental frequency of the shell	
	OMPL	Fundamental frequency of the plate	
	SHDEN	Density of shell material	
	PLDEN	Density of plate material	
		For a non-dimensional run: thicknesses, frequencies and densitites should be given as non-dimensional quantities as listed in Item 6, Table 1. Young's modulus and the implied unit p_0 value should have the same units.	
		For a dimensional run: material and structural densities should have the same units. Thicknesses, densities, moduli, frequencies and applied pressure should have consistent units of length, time and force.	
14	ILYR	The index of the line forming the lower boundary of the layer. See Fig. 6	one card containing 8 quantities, for
	DZ	Space increment in the Z-direction relative to R_0 .	Maximum number of cards = NLAYR
	LAMLD	Non-dimensional loading wave speed λ_L . See Table 1	I5,5X,7F10.0

TABLE 7 – NUMBERING OF VARIABLES FOR GRAPHIC OUTPUT OR PRINTED OUTPUT

	VARIABLE NUMBER	VARIABLE DESCRIPTION	
Structure	1	σ_r	Radial stress at the structure/material interface
	2	σ_z	Longitudinal Stress
	3	σ_{rz}	Shear stress
	4	V_r	Radial velocity
	5	V_z	Longitudinal velocity
	6	W_r	Radial displacement
	7	W_z	Longitudinal displacement
	8	J_1	First invariant of stress
	9	$\sigma_{\theta\theta}$	Hoop stress
Field	1	σ_r	Radial stress
	2	σ_z	Longitudinal stress
	3	σ_{rz}	Shear stress
	4	V_r	Radial velocity
	5	V_z	Longitudinal velocity
	6	J_1	First invariant of stress

Appendix B

LIST OF COMMON VARIABLE NAMES

AJ1	The first stress invariant, J_1 evaluated at points in the field.
AJ1MX	Last maximum compressive value of J_1
ALPHP, ALPHS	Values of α for plate and shell as defined in Table 1, Item 5.
APDSG	Load applied at each point on the interior of the shell.
ARLM1, ARLP, AZLP AZLP1, AZLS	Intermediate quantities used in computation for right angle at shell-plate interface. See Eqs. (21)-(24)
CLD	Coefficient array computed with loading P-wave parameters.
CS	Coefficient array computed with S-wave parameters
CUN	Coefficient array computed with unloading P-wave parameters.
CNR1---CNR12	Coefficients defined for computations of motion of shell-plate structrue as follows:

$$CNR1 = \omega_s^2 \Delta\tau \qquad CNR2 = \beta_s \Delta\tau \qquad CNR3 = \omega_p^2 \Delta\tau$$

$$CNR4 = \omega_p^2 \alpha_p \Delta\tau \qquad CNR5 = \frac{1}{1+\gamma} \quad \text{where } \gamma = \frac{D_p}{D_s} \frac{\Delta R}{\Delta z_{LC}} \frac{\omega_s^2}{\omega_p^2} r_{LC}$$

$$CNR6 = \frac{r_{LC}}{\gamma r_{LC-1}} \qquad CNR7 = \frac{\gamma}{1+\gamma} \qquad CNR8 = \beta_p \Delta\tau$$

$$CNR11 = \frac{\Delta r}{\Delta z_{LC}} \qquad CNR12 = \frac{1}{2\left[1+\left(\frac{\Delta r}{\Delta z_{LC}}\right)^2\right]}$$

DENS	Density of each layer, relative to a base value ρ.
DR	Increment of space in the R-direction; ΔR.
DR2, DR3, DR4	(ΔR), (ΔR), $(\Delta R)^4$.
DT	Δt Increment of time.
DZ	ΔZ Increment of space in the Z-direction. Possibly different for each layer
DZ2, DZ3, DZ4	$(\Delta Z)^2$, $(\Delta Z)^3$, $(\Delta Z)^4$.

D1RWR,D1RWZ,D2RWR D2RWZ,D3RWZ,D4RWZ	Intermediate quantities used in computing shell velocities in the R and Z directions. See Tables 3a, 3b, 4a, 4b.
EPL,ESH	Young's modulus for the plate and shell, respectively.
HPL,HSH	Thickness of the plate and shell respectively.
I	Index in the Z-direction measured from the top.
IFLPT	I-index of field point at which graph output is desired.
ILOAD	Indicator for type of loading. See Table 6, card set 2.
ILYR	I-index at the bottom of each layer.
IPTS	Total number of mesh points in the field, = IRIZ-IRZSH
IPR	I-index of point in the field at which printed output is desired.
IR	Maximum number of mesh points in the R-direction.
IRIZ	The product of IR and IZ.
IRSHL	Total number of points on the plate.
IRSP1	= IRSHL+1
IRZSH	The product of IRSHL and IZSHL
ISHPR	Index of point on shell at which printed output is desired.
ISHPT	Total number of points around the cavity = IRSHL+IZSHL-1.
ITGRF	Time index increment for graphs of time histories.
IZ	Maximum number of mesh points in the Z-direction.
IZSHL	Maximum number of points on the shell.
IZSP1	= IZSHL+1
JFLPT	J-index of field point at which graphic output is desired.
JPR	J-index of field point at which printed output is desired.

JPTS	Number of mesh points in the R-direction in the field between the shell and the outer boundary. JPTS = IR-IRSHL.
JO	Index in the R-direction measured from the origin.
KODES	Indicator for state of load, unload, reload. See Table 5.
LAMLD,LAMS,LAMUN	Non-dimensional wave speeds for loading P-waves, unloading P-waves and S-waves, respectively.
LINE	Index of line along which a space profile is to be plotted.
LR	Array LR(I) defines the number of mesh points to be included in the integration in the r-direction along each I-th horizontal line.
LRMX	Maximum values of LR.
LYRSH	Number of the layer in which the plate sits.
LZ	Array LZ(J) Defines the number of mesh points to be included in the integration in the z-direction along each J-th vertical line.
LZMX	Maximum values of LZ.
MTPT	Time step number at which space profile is to be plotted.
MXGRF	Total number of time histories desired for field points.
MXGRS	Total number of time histories desired for structure points.
MXPRF	Total number of space profiles desired.
NFLV	Field variable number for which graphic output is desired. See Table 7.
NGRPH	Indicator for graphic output or not. See Table 6, card set 4.
NLAYR	Total number of layers.
NODIM	Indicator for non-dimensional or dimensional results. See Table 6, card set 4.
NORIT	Indicator for right angle preservation at shell plate interface. See Table 6, card set 4.

NOSHL	Indicator for structure or no-structure lining the cavity.
NPAIR	Total number of field points for which printed output is desired.
NPRSH	Total number of points around cavity at which printed output is desired.
NPRT	Time step index increment at which printed output is desired.
NRORZ	Indicator for direction in which space profile is to be plotted. See Table 6, card set 11.
NSHPT	Index of the point on the structure at which a time history is to be plotted.
NSHV	Number of the structure variable for which a time history is to be plotted. See Table 7.
NTIME	Maximum number of time steps to be computed.
NULD	Poisson ratio for loading conditions. See Table 1, Item 4.
NUUN	Poisson ratio for unload-reload conditions. See Table 1, Item 4.
NVAR	Number of the field variable for which a space profile is to be plotted. See Table 7.
OMPL,OMSH	Fundamental frequencies ω_p,ω_s for plate and shell respectively. See Table 1, Item 6.
OM2PL, OM2SH	ω_p^2,ω_s^2
PLDEN,PLNU	Density and Poisson ratio for plate material.
R	Distance in the r-direction measured from the origin.
SGR	Radial stress, σ_r at points in the field.
SGZ	Longitudinal stress, σ_z, at points in the field.
SHAJ1	First invariant at the structure-field interface
SHDEN	Density of shell material.
SHL1,SHL2	Coefficients for shell computations, $SHL1=1+\alpha_s$, $SHL2=1-\alpha_s$.
SHNU	Poisson ratio of shell material.

SHSGR,SHSGZ,SHSRZ	Stresses σ_r, σ_z, σ_{rz} measured in the field at the structure-material interface.
SHVR,SHVZ	Velocities of points on the structure in the R- and Z-directions, respectively.
SHWR,SHWZ	Displacements of points on the structure in the R- and Z-directions, respectively.
TIME	Cumulative time value from start of computation.
VR, VZ	Velocities of points in the field in the R- and Z-directions, respectively.
Z	Distance measured in the Z-direction from the top boundary.

DISTRIBUTION LIST

DEPARTMENT OF DEFENSE

Assistant Secretary of Defense
Cmd., Cont., Comm. & Intell.
Department of Defense
ATTN: ODASD IA

Assistant to the Secretary of Defense
Atomic Energy
Department of Defense
ATTN: Honorable Donald R. Cotter
ATTN: COL R. N. Brodie

Director
Defense Advanced Research Proj. Agency
ATTN: STO
ATTN: NMRO
ATTN: PMO
ATTN: Technical Library

Director
Defense Civil Preparedness Agency
Assistant Director for Research
ATTN: Staff Dir. Resr. George N. Sisson
ATTN: Admin. Officer

Director
Defense Communications Agency
ATTN: CCTC/C672, Franklin D. Moore
ATTN: Code 930

Defense Documentation Center
Cameron Station
12 cy ATTN: TC

Director
Defense Intelligence Agency
ATTN: DT-1C
ATTN: DT-2, Wpns. & Sys. Div.
ATTN: Technical Library
ATTN: DB-4C2, Timothy Ross
ATTN: DB-4C1, Paul Castleberry
ATTN: DB-4C3

Director
Defense Nuclear Agency
ATTN: DDST
ATTN: TISI, Archives
3 cy ATTN: TITL, Tech. Library
2 cy ATTN: SPSS
2 cy ATTN: SPAS

Dir. of Defense Research & Engineering
Department of Defense
ATTN: S&SS (OS)

Commander
Field Command
Defense Nuclear Agency
ATTN: FCPR
ATTN: FCTMOF

Director
Interservice Nuclear Weapons School
ATTN: Document Control

DEPARTMENT OF DEFENSE (Continued)

Director
Joint Strat. Target Planning Staff, JCS
ATTN: JLTW-2
ATTN: STINFO, Library
ATTN: XPFS
ATTN: DOXT

Chief
Livermore Division, Field Command, DNA
Lawrence Livermore Laboratory
ATTN: FCPRL

Chief
Test Construction Division
Field Command Test Directorate
Defense Nuclear Agency
ATTN: FCTC

DEPARTMENT OF THE ARMY

Director
BMD Advanced Tech. Center
Huntsville Office
ATTN: CRDABH-S
ATTN: CRDABH-X

Program Manager
BMD Program Office
ATTN: CRDABM-NE

Commander
BMD System Command
ATTN: BDMSC-TEN, Noah J. Hurst

Director
Construction Engineering Research Lab.
ATTN: CERL-SL

Dep. Chief of Staff for Research Dev. & Acq.
Department of the Army
ATTN: DAMA(CS), MAJ A. Gleim
ATTN: DAMA-CSM-N, LTC G. Ogden
ATTN: Technical Library

Chief of Engineers
Department of the Army
ATTN: DAEN-MCE-D
ATTN: DAEN-RDM

Deputy Chief of Staff for Ops. & Plans
Department of the Army
ATTN: Dir. of Chem. & Nuc. Ops.
ATTN: Technical Library

Chief
Engineer Strategic Studies Group
ATTN: DAEN-FES, LTC Hatch

Commander
Harry Diamond Laboratories
ATTN: DRXDO-NP
ATTN: DRXDO-TI, Tech. Lib.

DEPARTMENT OF THE ARMY (Continued)

Commander
Picatinny Arsenal
ATTN: Technical Library
ATTN: DR-DAR-L-C-FA, B. Shulman

Commander
Redstone Scientific Information Center
US Army Missile Command
ATTN: Chief, Documents

Commander
US Army Armament Command
ATTN: Tech. Lib.

Director
US Army Ballistic Research Labs.
ATTN: DRXBR-X, Julius J. Meszaros
ATTN: Charles Kingery
2 cy ATTN: Tech. Lib., Edward Baicy
ATTN: W. Taylor
ATTN: A. Ricchiazzi
ATTN: DRDAR-BLE, J. H. Keefer

Commander
US Army Comb. Arms Combat Dev. Acty.
ATTN: LTC G. Steger
ATTN: LTC Pullen

Commander
US Army Communications Cmd.
ATTN: Technical Library

Commander
US Army Electronics Command
ATTN: DRSEL-TL-IR, Edwin T. Hunter

Commander
US Army Engineer Center
ATTN: ATSEN-SY-L

Division Engineer
US Army Engineer Div. Huntsville
ATTN: HNDED-SR

Division Engineer
US Army Engineer Div. Ohio River
ATTN: Technical Library

Commandant
US Army Engineer School
ATTN: ATSE-TEA-AD
ATTN: ATSE-CTD-CS

Director
US Army Engr. Waterways Exper. Sta.
ATTN: Leo Ingram
ATTN: Guy Jackson
ATTN: John N. Strange
ATTN: Technical Library
ATTN: William Flathau
ATTN: James Ballard

Commander
US Army Foreign Science & Tech. Center
ATTN: Research & Concepts Branch

DEPARTMENT OF THE ARMY (Continued)

Commander
US Army Mat. & Mechanics Research Center
ATTN: Technical Library
ATTN: John Mescall
ATTN: Richard Shea

Commander
US Army Materiel Dev. & Readiness Cmd.
ATTN: Technical Library
ATTN: DRCDE-D, Lawrence Flynn

Commander
US Army Missile Command
ATTN: DRSMI-XS, Chief Scientist
ATTN: J. Hogan

Commander
US Army Mobility Equip. R & D Center
ATTN: Al Tolbert
ATTN: Technical Library

Commander
US Army Nuclear Agency
ATTN: Tech. Lib.
ATTN: ATCA-NAW

Commander
US Army Training & Doctrine Command
ATTN: LTC J. Foss
ATTN: LTC Auveduti, COL Enger

Commandant
US Army War College
ATTN: Library

US Army Mat. Cmd. Proj. Mngr. for Nuc. Munitions
ATTN: DRCPM-NUC

DEPARTMENT OF THE NAVY

Chief of Naval Material
Navy Department
ATTN: MAT 0323

Chief of Naval Operations
Navy Department
ATTN: OP 03EG
ATTN: OP 981
ATTN: OP 982, CAPT Toole
ATTN: OP 982, LCDR Smith
ATTN: Code 604C3, Robert Piacesi
ATTN: OP 982, LTC Dubac

Chief of Naval Research
Navy Department
ATTN: John Haycock
ATTN: Nicholas Perrone
ATTN: Code 464, Thomas P. Quinn
ATTN: Code 464, Jacob L. Warner
ATTN: Technical Library

Officer in Charge
Civil Engineering Laboratory
Naval Construction Battalion Center
ATTN: Technical Library
ATTN: R. J. Odello
ATTN: Stan Takahashi

DEPARTMENT OF THE NAVY (Continued)

Commandant of the Marine Corps
Navy Department
ATTN: POM

Commander
David W. Taylor Naval Ship R & D Center
ATTN: Code L42-3, Library

Commanding General
Development Center
Fire Support Branch
MCDEC
ATTN: CAPT Hartneady
ATTN: LTC Gapenski

Commander
Naval Air Systems Command
Headquarters
ATTN: F. Marquardt

Commander
Naval Electronic Systems Command
Naval Electronic Systems Cmd. Hqs.
ATTN: PME 117-21A

Commanding Officer
Naval Explosive Ord. Disposal Fac.
ATTN: Code 504, Jim Petrousky

Commander
Naval Facilities Engineering Command
Headquarters
ATTN: Technical Library
ATTN: Code 04B
ATTN: Code 03A

Commander
Naval Ocean Systems Center
ATTN: Technical Library

Superintendent (Code 1424)
Naval Postgraduate School
ATTN: Code 2124, Tech. Rpts. Librarian

Director
Naval Research Laboratory
ATTN: Code 8440, F. Rosenthal
ATTN: Code 2600, Tech. Lib.

Commander
Naval Sea Systems Command
Navy Department
ATTN: ORD-033
ATTN: Code 03511
ATTN: ORD-91313, Lib.
ATTN: SEA-9931G

Commander
Naval Ship Engineering Center
Department of the Navy
ATTN: NSEC 6105G
ATTN: Technical Library

Commander
Naval Ship Research & Development Center
Underwater Explosive Research Division
ATTN: Technical Library

DEPARTMENT OF THE NAVY (Continued)

Commander
Naval Surface Weapons Center
ATTN: Code 240, C. J. Aronson
ATTN: M. Kleinerman
ATTN: G. L. Matteson
ATTN: Code WA501, Navy Nuc. Progms. Off.

Commander
Naval Surface Weapons Center
Dahlgren Laboratory
ATTN: Technical Library

President
Naval War College
ATTN: Technical Library

Commander
Naval Weapons Center
ATTN: Code 533, Tech. Lib.

Commanding Officer
Naval Weapons Evaluation Facility
ATTN: Technical Library
ATTN: R. Hughes

Director
Strategic Systems Project Office
Navy Department
ATTN: NSP-272
ATTN: NSP-43, Tech. Lib.
ATTN: NSP-273

DEPARTMENT OF THE AIR FORCE

Commander
ADCOM/XPD
ATTN: XP
ATTN: XPQDQ

AF Geophysics Laboratory, AFSC
ATTN: LWW, Ker C. Thompson
ATTN: SUOL, Research Lib.

AF Institute of Technology, AU
ATTN: Library AFIT, Bldg. 640, Area B

AF Weapons Laboratory, AFSC
ATTN: DEP, Jimmie L. Bratton
ATTN: DES-S, M. A. Plamondon
ATTN: DES-C, Robert Henny
ATTN: DED
ATTN: DES-G, Mr. Melzer
ATTN: SUL

Headquarters
Air Force Systems Command
ATTN: Technical Library
ATTN: DLCAW
ATTN: R. Cross

Commander
Armament Development & Test Center
ATTN: Tech. Library
ATTN: ADBRL-2

Commander
ASD
ATTN: Technical Library

DEPARTMENT OF THE AIR FORCE (Continued)

Assistant Secretary of the Air Force
Research & Development
Headquarters, US Air Force
ATTN: Col R. E. Steere

Deputy Chief of Staff
Research & Development
Headquarters, US Air Force
ATTN: Col J. L. Gilbert

Commander
Foreign Technology Division, AFSC
ATTN: ETDP
ATTN: PDBG
ATTN: NICD, Library
ATTN: PDBF, Mr. Spring

Hq. USAF/IN
ATTN: IN

Hq. USAF/PR
ATTN: PRE

Hq. USAF/RD
ATTN: RDQRM, Col S. C. Green
ATTN: RDQPN, Maj F. Vajda
ATTN: RDQSM
ATTN: RDPS, Lt Col A. Chiota
ATTN: RDPM

Commander
Rome Air Development Center, AFSC
ATTN: EMTLD, Doc. Library
ATTN: EMREC, R. W. Mair

SAMSO/DE
ATTN: DEB

SAMSO/DY
ATTN: DYS

SAMSO/MN
ATTN: MMH
ATTN: MNNH

SAMSO/RS
ATTN: RSS/Col Donald Dowler

SAMSO/XR
ATTN: XRTB

Commander in Chief
Strategic Air Command
ATTN: XPFS
ATTN: NRI-STINFO, Library

ENERGY RESEARCH & DEVELOPMENT ADMINISTRATION

Division of Military Application
US Energy Research & Dev. Admin.
ATTN: Doc. Con. for Test Office

Los Alamos Scientific Laboratory
ATTN: Doc. Con. for G. R. Spillman
ATTN: Doc. Con. for Reports Lib.
ATTN: Doc. Con. for Al Davis

ENERGY RESEARCH & DEVELOPMENT ADMINISTRATION (Continued)

University of California
Lawrence Livermore Laboratory
ATTN: D. M. Morris, L-90
ATTN: Tech. Info. Dept. L-3
ATTN: Ted Butkovich, L-200
ATTN: Larry W. Woodruff, L-96
ATTN: Richard G. Dong, L-90
ATTN: Jerry Goudreau
ATTN: M. Fernandez
ATTN: J. R. Hearst, L-205
ATTN: Jack Kahn, L-7
ATTN: Robert Schock, L-437

Sandia Laboratories
Livermore Laboratory
ATTN: Doc. Con. for Tech. Library

Sandia Laboratories
ATTN: Doc. Con. for A. J. Chaban
ATTN: Doc. Con. for M. L. Merritt
ATTN: Doc. Con. for Luke J. Vortman
ATTN: Doc. Con. for 3141, Sandia Rpt. Coll.
ATTN: L. Hill
ATTN: Doc. Con. for W. Roherty

US Energy Research & Dev. Admin.
Albuquerque Operations Office
ATTN: Doc. Con. for Tech. Library

US Energy Research & Dev. Admin.
Division of Headquarters Services
Library Branch G-043
ATTN: Doc. Con. for Class Tech. Lib.

US Energy Research & Dev. Admin.
Nevada Operations Office
ATTN: Doc. Con. for Tech. Lib.

Union Carbide Corporation
Holifield National Laboratory
ATTN: Doc. Con. for Tech. Lib.
ATTN: Civil Def. Res. Proj.

OTHER GOVERNMENT AGENCIES

Central Intelligence Agency
ATTN: RD/SI, Rm. 5G48, Hq. Bldg. for NED/OSI-5G48 Hqs.

Department of the Interior
Bureau of Mines
ATTN: Tech. Lib.

Department of the Interior
US Geological Survey
ATTN: J. H. Healy
ATTN: Cecil B. Raleigh

NASA
Ames Research Center
ATTN: Robert W. Jackson

Office of Nuclear Reactor Regulation
Nuclear Regulatory Commission
ATTN: Robert Heineman
ATTN: Lawrence Shao

DEPARTMENT OF DEFENSE CONTRACTORS

Aerospace Corporation
ATTN: Prem N. Mathur
ATTN: Larry Selzer
2 cy ATTN: Tech. Info. Services

Agbabian Associates
ATTN: M. Agbabian
ATTN: Carl Bagge

Analytic Services, Inc.
ATTN: George Hesselbacher

Applied Theory, Inc.
2 cy ATTN: John G. Trulio

Artec Associates, Inc.
ATTN: Steven Gill

Avco Research & Systems Group
ATTN: William Broding
ATTN: Research Lib., A830, Rm. 7201

Battelle Memorial Institute
ATTN: Technical Library
ATTN: R. W. Klingesmith

The BDM Corporation
ATTN: A. Lavagnino
ATTN: Technical Library

The BDM Corporation
ATTN: Richard Hensley

Bell Telephone Laboratories
ATTN: J. P. White

The Boeing Company
ATTN: R. H. Carlson
ATTN: Robert Dyrdahl
ATTN: Aerospace Library

Brown Engineering Company, Inc.
ATTN: Manu Patel

California Institute of Technology
ATTN: Thomas J. Ahrens

California Research & Technology, Inc.
ATTN: Technical Library
ATTN: Ken Kreyenhagen
ATTN: Sheldon Shuster

University of California
Berkeley Campus Room 318
Sproul Hall
ATTN: G. Sachman

Calspan Corporation
ATTN: Technical Library

Center for Planning & Research, Inc.
ATTN: R. W. Shnider

Civil/Nuclear Systems Corp.
ATTN: Robert Crawford

University of Dayton
Industrial Security Super KL-505
ATTN: Hallock F. Swift

DEPARTMENT OF DEFENSE CONTRACTORS (Continued)

University of Denver
Colorado Seminary
Denver Research Institute
ATTN: Sec. Officer for J. Wisotski

EG & G, Inc.
Albuquerque Division
ATTN: Technical Library

Electric Power Research Institute
ATTN: George Sliter

Electromechanical Sys. of New Mexico, Inc.
ATTN: R. A. Shunk

Engrg. Decision Analysis Co., Inc.
ATTN: R. P. Kennedy

The Franklin Institute
ATTN: Zenons Zudans

Gard, Incorporated
ATTN: G. L. Neidhardt

General Dynamics Corp.
Pomona Division
ATTN: Keith Anderson

General Dynamics Corp.
Electric Boat Division
ATTN: Michael Pakstys

General Electric Company
Space Division
Valley Forge Space Center
ATTN: M. H. Bortner, Space Sci. Lab.

General Electric Company
Re-Entry & Environmental Systems Div.
ATTN: Arthur L. Ross

General Electric Company
TEMPO-Center for Advanced Studies
ATTN: DASIAC

General Research Corporation
ATTN: Benjamin Alexander

Geocenters Incorporated
ATTN: Edward Marram

H-Tech. Laboratories, Inc.
ATTN: B. Hartenbaum

Honeywell Incorporated
Defense Systems Division
ATTN: T. N. Helvig

IIT Research Institute
ATTN: Technical Library
ATTN: R. E. Welch

Univ. of Illinois at Chicago
College of Engineering
Dept. of Materials Engineering
ATTN: Ted Belytschko

Institute for Defense Analyses
ATTN: IDA Librarian, Ruth S. Smith

DEPARTMENT OF DEFENSE CONTRACTORS (Continued)

J. H. Wiggins, Company, Inc.
ATTN: Jon Collins

Kaman AviDyne
Division of Kaman Sciences Corp.
ATTN: Technical Library
ATTN: E. S. Criscione
ATTN: Norman P. Hobbs

Kaman Sciences Corporation
ATTN: Frank H. Shelton
ATTN: Paul A. Ellis
ATTN: Library

Karagozian & Case
ATTN: John Karagozian

Lockheed Missiles & Space Company, Inc.
ATTN: Technical Library

Lockheed Missiles & Space Company, Inc.
ATTN: Tom Geers, D/52-33, Bldg. 205

Lovelace Foundation for Medical Educ. & Rsch.
ATTN: Technical Library
ATTN: Asst. Dir. of Res., Robert K. Jones

Martin Marietta Aerospace
Orlando Division
ATTN: G. Fotieo

McDonnell Douglas Corporation
ATTN: Robert W. Halprin

McMillian Science Associates, Inc.
ATTN: Robert Oliver

Merritt Cases, Incorporated
ATTN: J. L. Merritt
ATTN: Technical Library

Meteorology Research, Inc.
ATTN: William D. Green

The Mitre Corporation
ATTN: Library

University of New Mexico
Dept. of Campus Security & Police
ATTN: G. E. Triandafalidis

Nathan M. Newmark
Consulting Engineering Services
B106A Civil Engineering Building
University of Illinois
ATTN: Nathan M. Newmark

Pacifica Technology
ATTN: G. Kent
ATTN: R. Bjork

Physics International Company
ATTN: Doc. Con. for Larry A. Behrmann
ATTN: Doc. Con. for E. T. Moore
ATTN: Doc. Con. for Coye Vincent
ATTN: Doc. Con. for Dennis Orphal
ATTN: Doc. Con. for Robert Swift
ATTN: Doc. Con. for Tech. Lib.
ATTN: Doc. Con. for Fred M. Sauer
ATTN: Doc. Con. for Charles Godfrey

DEPARTMENT OF DEFENSE CONTRACTORS (Continued)

Prototype Development Associates, Inc.
ATTN: T. K. McKinley

R & D Associates
ATTN: Henry Cooper
ATTN: Harold L. Brode
ATTN: Arlen Fields
ATTN: Paul Rausch
ATTN: Cyrus P. Knowles
ATTN: Albert L. Latter
ATTN: William B. Wright, Jr.
ATTN: Robert Port
ATTN: Technical Library
ATTN: Jerry Carpenter
ATTN: J. G. Lewis

The Rand Corporation
ATTN: Armas Laupa
ATTN: Technical Library
ATTN: C. C. Mow

Science Applications, Inc.
ATTN: D. E. Maxwell
ATTN: David Bernstein

Science Applications, Inc.
ATTN: Technical Library

Science Applications, Inc.
ATTN: James Cramer

Science Applications, Inc.
ATTN: Steve Oston

Science Applications, Incorporated
ATTN: William M. Layson
ATTN: Burt Chambers

Southwest Research Institute
ATTN: A. B. Wenzel
ATTN: Wilfred E. Baker

Stanford Research Institute
ATTN: George R. Abrahamson

Systems, Science & Software, Inc.
ATTN: Robert Sedgewick
ATTN: Thomas D. Riney
ATTN: Donald R. Grine
ATTN: Ted Cherry
ATTN: Technical Library

Terra Tek, Inc.
ATTN: Technical Library
ATTN: Sidney Green
ATTN: A. H. Jones

Tetra Tech., Inc.
ATTN: Li-San Hwang
ATTN: Technical Library

Texas A & M University System
Texas A & M Research Foundation
ATTN: Harry Coyle

TRW Defense & Space Sys. Group
ATTN: Tech. Info. Center/S-1930
ATTN: Norm Lipner
2 cy ATTN: Peter K. Dai, R1/2170
ATTN: Donald Jortner, R1-2144
ATTN: Pravin Bhutta, R1-1104

DEPARTMENT OF DEFENSE CONTRACTORS (Continued)

TRW Defense & Space Sys. Group
San Bernardino Operations
ATTN: F. Y. Wong, 527/712

TRW Defense & Space Sys. Group
ATTN: Gregory D. Hulcher

Universal Analytics, Inc.
ATTN: F. I. Field

URS Research Company
ATTN: Technical Library
ATTN: Ruth Schneider

The Eric H. Wang
Civil Engineering Research Fac.
University Station
ATTN: Larry Bickle
ATTN: Neal Baum

DEPARTMENT OF DEFENSE CONTRACTORS (Continued)

Washington State University
Administrative Organization
ATTN: Arthur Miles Hohorf for George Duval

Weidlinger Assoc. Consulting Engineers
ATTN: J. M. McCormick
ATTN: Melvin L. Baron
ATTN: A. T. Matthews
ATTN: H. H. Bleich

Weidlinger Assoc. Consulting Engineers
ATTN: J. Isenberg

Westinghouse Electric Corp.
Marine Division
ATTN: W. A. Volz